

**SLOVAK UNIVERSITY OF TECHNOLOGY
IN BRATISLAVA**

FACULTY OF CHEMICAL AND FOOD TECHNOLOGY

Reg. No.: FCHPT-FCHPT-16584-104148

Modelling and Optimal Operation of a Forward Osmosis Process

MASTER THESIS

2024

Bc. Matej Ružička

**SLOVAK UNIVERSITY OF TECHNOLOGY
IN BRATISLAVA**

FACULTY OF CHEMICAL AND FOOD TECHNOLOGY

Reg. No.: FCHPT-FCHPT-16584-104148

Modelling and Optimal Operation of a Forward Osmosis Process

MASTER THESIS

Study programme: Automation and Information Engineering in Chemistry and Food Industry
Study field: Cybernetics
Training workspace: Institute of Information Engineering, Automation and Mathematics
Thesis supervisor: doc. Ing. Radoslav Paulen, PhD.

2024

Bc. Matej Ružička



MASTER THESIS TOPIC

Student: **Bc. Matej Ružička**
Student's ID: 104148
Study programme: Automation and Information Engineering in Chemistry and Food Industry
Study field: Cybernetics
Thesis supervisor: doc. Ing. Radoslav Paulen, PhD.
Head of department: doc. Ing. Martin Klaučo, PhD.
Workplace: Department of Information Engineering and Process Control FCHPT
STU, Aquaporin A/S

Topic: **Modelling and Optimal Operation of a Forward Osmosis Process**

Language of thesis: English

Specification of Assignment:

Membrane separation is one of the most modern and cost-effective separation processes in the chemical and biochemical industry. The goal of this project is to create a mathematical model of the forward osmosis process, estimate the parameters of the model from the measured data, verify the correctness of the designed model and propose the optimal operation of the plant.

Selected bibliography:

1. Foley, G.. Membrane Filtration: A Problem Solving Approach with MATLAB. Cambridge University Press. 2013. ISBN 978-1-107-62746-8
2. KHAN, M. A. W.; Zubair, M. M.; Saleem, H.; AlHawari, A.; Zaidi, S. J.. Modeling of osmotically-driven membrane processes: An overview. Desalination, 117183. 2023.

Deadline for submission of Master thesis: 12. 05. 2024

Approval of assignment of Master thesis: 26. 02. 2024

Assignment of Master thesis approved by: prof. Ing. Miroslav Fikar, DrSc. – study programme supervisor

Contents

1	Introduction	9
2	Problem Description	13
3	Problem Solution	17
3.1	Process Modelling	17
3.2	Model Fitting	19
3.2.1	White Box Approach	20
3.2.2	Grey Box Approach	20
3.2.3	Black Box Approach	21
3.3	Process optimisation	22
4	Results	27
4.1	Flux Models	28
4.1.1	FO Model Design – White Box Approach	28
4.1.2	FO Model Design – Black Box Approach	28
4.1.3	FO Model Design – Grey Box Approach	37
4.1.4	Grey box vs Black box results comparison	43
4.2	Model Validation	43

4.3 RO Flux Model Derivation	47
4.4 Process Optimisation	48
5 Conclusions and Future Research	65
Bibliography	69
Resumé	71

Honour Declaration

I declare that the submitted diploma thesis was completed on my own, in cooperation with my supervisor, with the help of professional literature and other information sources, which are cited in my thesis in the reference section. As the author of my diploma thesis, I declare that I didn't break any third party copyrights.

.....

Signature

Acknowledgement

I am deeply grateful to my supervisor Dr. Radoslav Paulen for his invaluable guidance, patience, and wealth of knowledge throughout my master's thesis, as well as for providing me with the opportunity to present partial results on scientific conferences. Additionally, I extend my thanks to my mentor, Dr. Ingrid Helgeland for her support, practical experience and guidance during my internship in Aquaporin A/S, where I was firstly introduced to the problem that my thesis focuses on.

Abstract

The forward osmosis (FO) process, despite being less established compared to reverse osmosis (RO), holds significant potential for water purification and solutions concentration due to its reliance on natural osmotic pressure. By utilising a membrane module and feed and draw solutions, FO facilitates water separation through osmotic pressure differences, offering benefits like feed solution harmlessness and energy savings. Through mathematical modelling, we can anticipate system dynamics, compare modelling approaches, and optimise the process to achieve desired outcomes with minimal energy input. Simulations of the optimised process provide insights into its behaviour, enabling operators to make real-time adjustments as needed.

Keywords: Forward osmosis, Reverse Osmosis, Process Modelling, Process Optimisation, Process Simulation

Abstrakt

Napriek tomu, že proces doprednej osmózy (FO) je priemyselne menej etablovaným v porovnaní s reverznou osmózou (RO), jeho potenciál v oblasti čistenia a koncentrácie roztokov je vďaka jeho funkčnému mechanizmu veľmi perspektívny. Využitím membránového modulu a tzv. odľahového roztoku umožňuje FO separáciu vody na princípe rozdielu osmotického tlaku medzi zakonzentrovaným a odľahovým roztokom. To zapríčiňuje výhody z hľadiska šetrnosti voči vstupným roztokom a úsporu energie. Matematickým modelovaním môžeme predpovedať dynamiku systému a optimalizovať ho z hľadiska vyžadovaných kvalitatívnych parametrov. Vytvorenie simulácie optimalizovaného procesu poskytuje operátorom pohľad na správanie systému a adekvátne naň podľa potreby reagovať.

Kľúčové slová: Dopredná osmóza, Reverzná osmóza, Modelovanie, Optimalizácia procesu, Simulácia

Introduction

Membrane technology is well established in process industry mostly for purification and concentration of solutions. A popular membrane process, e.g. for seawater desalination and various forms of aqueous solutions treatments, is reverse osmosis (RO). The principle of reverse osmosis process involves the use of a semi-permeable membrane to separate water from the feed to get either purified water (marked as permeate) or concentrated feed solution (retentate). Input feed solution is pushed through the membrane under high pressure, allowing only pure water molecules to pass while blocking all the other dissolved and non-dissolved solutes. In some cases this high external hydraulic pressure causes devaluation of feed due to the increase of temperature or mechanical impact. The other problem that RO process faces is when the feed is an aqueous mixture containing particles which might congest membrane pores or damage a membrane completely [5].

RO cannot be applied in some specific conditions, for example in aircraft or spacecraft. Water separation is needed there for fresh water production. RO is also unsuitable for concentration of some food beverages as the external pressure could damage its components. Usage of membranes of higher quality might help. In membrane technologies, RO membranes represent thin porous layer permeable for water and not for solutes. That is why they are marked as semi-permeable. They are composed of polymers like polyamide, polypropylene, polysulfone and other mostly synthetic macromolecules. Discovery of aquaporin proteins, naturally present in biological cells has significantly contributed to the development of alternative to RO membrane technology [6]. Hollow fibre membranes containing aquaporin proteins are these type of quality membranes which are naturally present in biological cells. They have prompted researchers to explore water purification to find similar alternative membrane technology which would serve as a complement to RO. One which would be applicable in conditions which are not for RO. Such conditions as for example those already mentioned — concentration of pressure sensitive solutions. For this purpose, process known as forward osmosis (FO) has been designed. The main inspiration in

searching for this new method was nature. Every living cell works on the principal of forward osmosis. Compared to RO, the forward osmosis process is a less established membrane technology [11]. Its potential is though vast in water purification and solutions concentration. In FO, the separation is based on a natural osmotic pressure. The main difference between these two similar membrane technologies enables various benefits for application of FO such as harmless to feed solutions and promising energy savings.

As the natural osmotic pressure is used as a driving force, the process is not harmful at all. That is why it is used in cases when we want components of the mixture (out of which is water separated) to remain untouched. Such processes represent concentrating of liquid foods and beverages, such as fruit juices. Without applying excessive pressure or high temperatures they retain flavours and nutrients. FO is therefore applied in the pharmaceutical sphere for the purpose of separation of sensitive compounds. It is gentler on certain bio molecules and sensitive compounds and so it preserves their molecular integrity. [13]

To stand up to the expectations, the FO plants need to be optimally designed and operated [2]. For this purpose, mathematical modelling is needed to reveal characteristic (static and dynamic) behaviour of the process under different design and operational decisions. One of the biggest challenges in membrane process modelling is to reliably predict the membrane flux, because that is a physical quantity describing a performance of the process's main purpose - water separation from the feed. It determines the dynamics of feed concentration increase, feed volume decrease and also dynamics of other process states. Therefore it is important to be able to estimate its future behaviour by finding its model. Although mass transfer theory provides several well understood mechanisms and theoretical foundations, it is often indicated that the experimenters encounter deviations from the ideal (theoretical) behaviour. Aim is to come up with such modelling approach which will predict the real behaviour of the process most accurately [10].

While having a model is a necessary condition for optimising the process, it is not the only requirement. To optimise the process effectively, we must also consider the material and energy load that the process entails in a given setup, including factors such as CAPEX (capital expenditure, representing physical — material funds of the process) and OPEX (operating expenditure, in this case representing energetic demand). Additionally, it is crucial to understand how quickly the process needs to operate to achieve the desired results. Comparing the study of the process characteristics such as quality, energy load and dynamics is crucial for the optimisation from the economical point of view. By that is meant answering of questions such as: Is it more

economically efficient to run the process for a longer duration while saving half of the overall energy required or is it economically less-demanding to equip more process components, such as another membranes to get the desired product quicker while preserving the same energy load. Alternatively, is the product sufficiently valuable to justify a more expensive, quicker-earning mechanism? All of these considerations must be taken into account when optimising the process from an economic standpoint. In our work, we will concentrate on optimising from operational, temporal, and qualitative perspectives. That is a crucial part for consequent overall economical optimisation. This economical site will be subject of our further research.

As mentioned above, forward osmosis (FO) is less established membrane technique compared to reverse osmosis (RO). However, in recent years, it has proven to be a highly promising and energy-efficient water treatment technology (mainly waste water purification, concentration of aqueous solutions). In our case we will focus on this second application — concentration of beverages. Concretely, our aim is to design an optimal FO process setup to increase the concentration of orange juice to the desired level. By considering all the economic aspects, we determine the optimal operational setup of the process.

Numerous studies have been conducted to reflect ongoing advancements in membrane development, process optimisation, and environmental sustainability. Various modelling approaches have been implemented providing different results, alongside testing of different setups and process modifications. Each study focused on a slightly different process and served a unique purpose [9]. Our contribution to this field lies in the comparison of distinct, individually selected modelling approaches, which integrate theoretical knowledge with experimentally derived data. Using these approaches, we can then optimise the process the way that it fits best our studied process. Because generally known modelling approaches are not appropriate for our case. That is why it is meaningful to come up with our unique modelling methods. Additionally, we provide simulations of the optimised process to visualise its behaviour. This allows operators to observe the entire time evolution and actively adjust inputs as needed.

Problem Description

FO Process Design

The FO process essentially consists of three main parts, which are feed module (FO membrane, feed tank), draw solution tank, and a draw recovery system which is in most cases represented by reverse (RO) or high-pressure reverse (HPRO) osmosis. RO module includes membrane (which can withstand high pressures, depending on our concentration goal) and a pump which generates external pressure forcing the water molecules inside the draw solution to pass across the membrane [14]. That is the component, energy demand of which we aim to minimize. Draw recovery system does not necessarily need to be maintained by the reverse osmosis system. [8] publishes an article in which he describes the process of regenerating the concentration of draw solution composed of ethylenediaminetetraacetic acid disodium (EDTA-2Na) molecules by acidification with HCl in an ice bath and consequent filtration followed by drying of the solution.

But, as mentioned above, in our case we use as a draw recovery system reverse osmosis which divides the system into two sections - RO and FO. Therefore it can be also marked as a hybrid system. Both parts are characterised by different form of osmotic water transport mechanism [14]. The process system is schematically depicted in Figure 2.1. It is important to emphasise the fact that we are discussing the batch setup of the process, not the continuous one. The main condition that needs to be maintained for the FO process to function is to have the osmotic pressure of the draw solution much higher than the osmotic pressure that the feed solution aims to reach. For our purpose we use K-lac (potassium lactate) as a draw solute. This gives a prerequisite for establishing a driving force for the separation of water from the feed, i.e., osmotic pressure difference. An FO membrane module, provides an interface between the feed and draw solutions. By design and thanks to the natural phenomena, water passes from the feed to the draw solution. As a result, the feed solution gets concentrated.

Consequently, draw solution gets diluted and needs to be recovered for the effective continuation of the process.

For this purpose, an RO membrane module is placed in the system. As mentioned above, for the separation of water to occur through the RO membrane, external pressure is required. This is supplied by an RO pump (which is not the same as the pumps which deliver feed or draw solution to membranes. It is the pump which forces the water molecules to flow from the area of higher concentration — diluted draw solution, to less concentrated area — fresh water on the other side of the membrane). Final products of the process are purified water and concentrated feed. Furthermore, it should be noted that the materials of the used membranes and composition of the draw tank are selected appropriately, the separation of water from the draw solution (regeneration of the draw solution) is more energy efficient than using the RO directly for the feed solution [14].

As mentioned above, our objective in modelling the system is to predict its behaviour. To achieve this, we utilise physical laws describing each sub-process of the system. This modelling method is referred to as a white box approach, as all of the principles are theoretical, general, and transparent (by which is meant that the mathematical laws and equations are well-known). However, the limitation of this modelling approach is that it predicts the process well only under ideal conditions, which are rarely maintained in real cases. Therefore, data-based modelling is a more commonly practised approach [10].

Data-based modelling is a method applied in the process industry to predict and understand the manner of intricate systems. This method involves collecting of the measured values from the system, creating a model based on these data, and using the model to forecast the system's future manner. Advantages of this approach include the identification of trends and patterns in the data, optimisation of process control, and improvement of the system's efficiency and effectiveness [10]. By having the knowledge about the flux model we are able to simulate the FO process which helps us understand it much better. Finding the optimal setup from the perspective of time, demand and quality is our main goal.

It is not only the design of the process chemical side (the used membrane and draw solution materials) that contributes to the overall energy efficiency. The process should be designed (decisions should be made on types and sizes of membrane modules, used pumps and tanks) and operated in an optimal manner. The optimal operation should take into account dynamic behaviour of the system. One should decide whether the draw tank should be kept in a steady-state condition (water removal through the RO

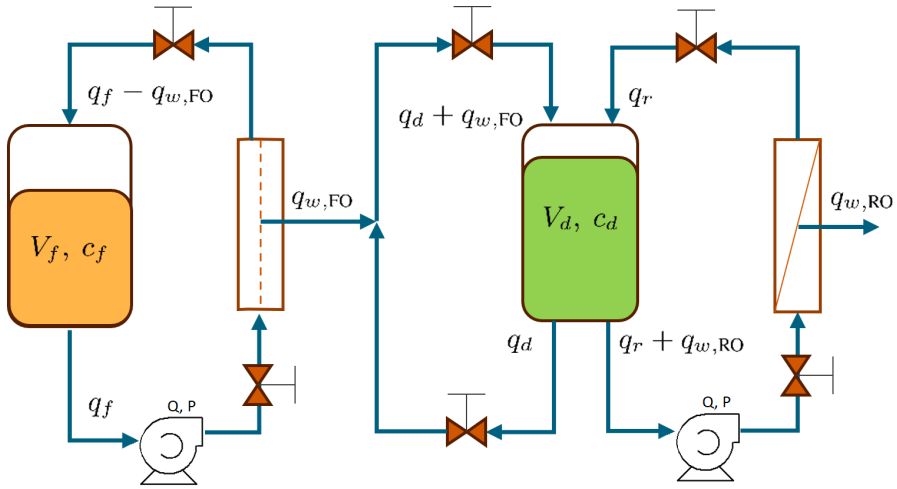


Figure 2.1: Scheme of the forward osmosis process.

module equal to the water flow through FO module) or whether the system should operate in some form of a cyclic regime (e.g., switching the separation through the RO on/off periodically). Mathematical model of the process is developed to help understand also this problem.

Besides deriving the model describing the system's behaviour we also provide information about its optimal setup. The system's energy consumption, time, and level of feed concentration are being taken into account. By knowing the working principle of RO part we are able to anticipate time and energy needed to get the desired concentration of the feed. We can also inform about the necessity of applying given amount of membranes for given long time period to be able to reach desired concentration level.

Goal

Because of the fact that FO process is still not that well established as an industrial process, our aim is to study. By that is meant:

- Finding of relations between inputs and outputs
- Learning how to estimate process states using principles of mathematical modelling
- Optimise the process from qualitative, temporal, and energetic standpoints

- Simulate the entire process based on selected models, inputs, scenarios, and optimisation preferences

The creation of a simulation provides a manual for easily anticipating productivity and the effectiveness of the process without the need to run it. Applying it we are therefore able to save material and energy.

Problem Solution

3.1 Process Modelling

For the development of a mathematical model, we assume perfect mixing in the tanks, fully developed hydraulic profiles, ideal membrane rejection (perfect passage of water and no passage of other substances), and common and constant temperature and density of all streams. We use the following notation. Indexes w , f , d , FO, and RO stand for water, feed, draw, forward and reverse osmosis, respectively. V stands for the volume (in L), q for flowrate (in L/h), J for permeate flux (in LMH, i.e., L/m²/h), A for the area of a membrane (in m²), ΔP for the transmembrane pressure (in bar), and c for the concentration (in kg/L), $\rho_f(c_f)$ for feed density which is a function of feed concentration. In our simplified model (Eq. (3.1)) we firstly assume the density to be constant — not related with feed concentration — constant density case. Mass balance of the system in Figure 2.1 is then read as:

$$\frac{dV_f(t)}{dt} = -q_{w,FO}(t) = -A_{FO}J_{w,FO}(c_f(t), c_d(t)), \quad (3.1a)$$

$$\frac{dV_d(t)}{dt} = q_{w,FO}(t) - q_{w,RO}(t) = A_{FO}J_{w,FO}(c_f(t), c_d(t)) - A_{RO}J_{w,RO}(c_d(t), \Delta P), \quad (3.1b)$$

$$\frac{dc_f(t)}{dt} = \frac{c_f(t)}{V_f(t)} A_{FO}J_{w,FO}(c_f(t), c_d(t)), \quad (3.1c)$$

$$\frac{dc_d(t)}{dt} = \frac{c_d(t)}{V_d(t)} [A_{FO}J_{w,FO}(c_f(t), c_d(t)) - A_{RO}J_{w,RO}(c_d(t), \Delta P)]. \quad (3.1d)$$

To design more accurate FO model, model of density is considered (Eq. (3.2)). Using literature data [12] we have derived a quadratic model describing relation between density of an orange juice and its concentration in brines. We mark it as Variable density case (Eqs. (3.3a) – (3.4)):

$$\rho_f(c_f(t)) = 0.0053c_f^2(t) + 4.3587c_f(t) + 1000 \quad (3.2a)$$

As we know from the theory, aquaporins selectively transmit water molecules, permeate is therefore pure water. For mass of permeate we can then write: $m_{\text{permeate}} = \rho_{\text{H}_2\text{O}} V_{\text{permeate}}$

$$\begin{aligned} \frac{d(\rho_f(c_f(t))V_f(t))}{dt} &= \rho_f(c_f(t)) \frac{dV_f(t)}{dt} + dV_f(t) \frac{d(\rho_f(c_f(t)))}{dt} = \\ -q_{w,\text{FO}}(t) &= -A_{\text{FO}} J_{w,\text{FO}}(c_f(t), c_d(t)) \rho_{\text{H}_2\text{O}} \end{aligned} \quad (3.3a)$$

To derive the change in feed volume over time, we utilize (3.3a). By a simple algebraic operation (subtracting the second element of the sum on the right-hand side of (3.3a) and dividing by $\rho_f(c_f(t))$), we obtain (3.4) below.

$$\frac{dV_f(t)}{dt} = \frac{-A_{\text{FO}} J_{w,\text{FO}}(c_f(t), c_d(t)) \rho_{\text{H}_2\text{O}} - V(t) \frac{d\rho_f(c_f(t))}{dt} \frac{dc_f(t)}{dt}}{\rho_f(c_f(t))} \quad (3.4)$$

Through similar algebraic operations as for the first state, we can derive a differential equation for the third state, denoted as c_f in equation (3.1c). One of the considerations we use in the derivations (3.5a) – (3.5d) of $\frac{dc_f(t)}{dt}$ is the law of mass preservation. As mentioned in equation (3.4), permeate leaving the feed tank is pure water. Therefore, the molar mass of solute remains constant in the feed tank, leading to zero change of $m_f c_f$ over time. The sequence of partial equations detailing the derivation process leading to the final equation for the feed volume over time is presented in equations (3.5a) – (3.5d).

$$\frac{d(m_f(t)c_f(t))}{dt} = m_f \frac{dc_f(t)}{dt} + c_f \frac{dm_f}{dt} = \frac{d(m_f(t)c_f(t))}{dt} = m_f \frac{c_f(t)}{dt} + c_f \frac{m_f}{dt} = 0 \quad (3.5a)$$

$$\rho_f(c_f(t))V_f(t) \frac{dc_f(t)}{dt} + c_f(t) \frac{d(\rho_f(c_f(t))V_f(t))}{dt} = 0 \quad (3.5b)$$

$$\rho_f(c_f(t))V_f(t) \frac{dc_f(t)}{dt} + c_f \rho_f(c_f(t)) \frac{dV_f}{dt} + c_f(t)V_f(t) \frac{d\rho_f(c_f(t))}{dt} = 0 \quad (3.5c)$$

$$\frac{dc_f(t)}{dt} = \frac{c_f(t)J_{w,\text{FO}}(c_f(t), c_d(t)) \rho_{\text{H}_2\text{O}}}{\rho_f(c_f(t))V_f(t) + c_f(t)V_f(t) \frac{d\rho_f(c_f(t))}{dt} - V \frac{d\rho_f(c_f(t))}{dt}} \quad (3.5d)$$

These more accurate differential equations derived from mass balances, where we do not assume the density of orange juice to be the same as water and not influenced by its concentration, will be included into our model.

The commonly used models for water flux through forward and reverse osmosis membranes can be obtained from the literature [10] as:

$$J_{w,FO}(c_f(t), c_d(t)) = k_w(\pi_d(c_d(t)) - \pi_f(c_f(t))), \quad (3.6)$$

$$J_{w,RO}(c_d(t), \Delta P) = k_w(\Delta P - \pi_d(c_d(t))), \quad (3.7)$$

where, k_w represents water permeability, determined experimentally based on water flux values under specific pressures for pure water (4.12). This experiment aimed to establish a simplified univariate model, maintaining constant pressure (in our case, approximately 100 bar). Although constant pressure values may not be anticipated in our application, this approach is essential for estimating the k_w parameter. This parameter is determined as an intercept in the model for flux through the RO membrane, dependent on the draw solution concentration. Further details of the experiment are discussed in 4.3.

The osmotic pressure π can be modelled as [7]:

$$\pi(c) = iRTc = -RT \ln \frac{a_w}{V_{H_2O}^m} \quad (3.8)$$

where i is the van't Hoff factor, R is the gas constant, and T is the temperature, a_w and water activity coefficient, $V_{H_2O}^m$ represents volume in m^3 of one kmol of H_2O what stands for $0.018m^3/kmol$. Its alternative definition is via water activity coefficient [13].

After the model has been successfully designed, the optimisation process takes place. In our case we will focus on minimisation of energy consumption of draw recovery system of FO process. As mentioned in the previous chapter 1 it is represented by RO membrane, purpose of which is to generate pressure high enough to extract water from diluted draw solution. By that it increases its concentration until it reaches regenerated state. This is the reason why the process costs energy input. For the work done by the pump we can write:

$$W = \int E(t) dt = Q\Delta P \quad (3.9)$$

where E stands for energy Q represents flow running through the pump.

3.2 Model Fitting

In our work, we employ white box (first-principles, theoretical model), grey box (first-principles model fitted with experimental data) and black box (simple regression model) principles to identify a mathematical model of an FO process.

3.2.1 White Box Approach

The mathematical models presented in Eqs. (3.1), (3.3a) represent a first-principles model. Using a white-box modelling principle, one can plug in the parameter values to obtain a final instance of the model ready for simulation, optimisation, etc. A common situation in practice is that the simplifications made by the process modelling assumptions result in inadequacies when model simulation results are compared to the experimental measurements. Equations taken from literature are the ones on which is the model of the system built on. They also serve as a predisposition to empirical modelling approaches (see below). Mathematical structure of these empirical models is derived out of them.

3.2.2 Grey Box Approach

To counteract the inadequacies of white box models a grey box modelling approach [4] has been designed as an alternative. This amounts to selecting an altered functional form of certain phenomena in the developed model while respecting the fundamental laws such as mass balances. In the case of FO process modelling, we opt for parameterising the permeate flux by a polynomial in $c_f(t)$ and $c_d(t)$. When deciding about the type of a polynomial function to use we need to follow the fundamental principles (white box). The model should be as simple as possible to avoid over-fitting, while also adhering to physical laws and trends, and accurately reflecting the real situation. This characteristic is evaluated by comparing estimated data from the model with measured data, using a validation dataset.

Assuming an experiment conducted over a certain time period with the permeate fluxes, volumes, and concentrations being measured, one can train the grey box model as a solution to:

$$\min_p \sum_{k=1}^N \sum_{m \in \{\text{FO}, \text{RO}\}} \frac{(J_{w,m}^{\text{exp}}(t_k) - J_{w,m}(t_k))^2}{2\lambda_{J_{w,m}}^2} + \sum_{s \in \{f,d\}} \frac{(V_s^{\text{exp}}(t_k) - V_s(t_k))^2}{2\lambda_{V_s}^2} + \frac{(c_s^{\text{exp}}(t_k) - c_s(t_k))^2}{2\lambda_{c_s}^2} \quad (3.10a)$$

$$\text{s.t. } J_{w,\text{FO}}(c_f(t), c_d(t)) = f_{w,\text{FO}}(c_f^{\text{exp}}(t), c_d(t), p), \quad (3.10b)$$

$$J_{w,\text{RO}}(c_d(t), \Delta P) = f_{w,\text{RO}}(c_d(t), \Delta P, p). \quad (3.10c)$$

where N is the number of experimental measurements, upper index exp denotes the measured values and λ is the standard deviation of the measurement noise. Conditions (3.10a) involve mass balance equations as well as initial conditions of the states, which can also be estimated. Equations (3.10b) and (3.10c) represent polynomials of

an appropriate order, derived from white box approach, whose parameters p are to be estimated. These coefficients stand in front of each independent variable in the flux model. They are found by solving the loss function (3.10). Due to the presence of differential equations Eqs. (3.1a)–(3.1d), (3.10) results in a dynamic optimisation problem.

3.2.3 Black Box Approach

The black box approach is another alternative, used when the mass balance cannot be reliably established, for example, due to missing information on system inflows and outflows. In such cases, a prediction model for water flux through a membrane can be formed similarly to the grey box approach, but without including mass balance equations in the model. It is much simpler than the grey box approach, but at the same time less realistic since it does not adhere to mass balances. It involves solving a loss function containing only the flux variable. As a result, the coefficients p found are of different values, as they are derived differently. The black box approach is derived as follows:

$$\min_p \sum_{k=1}^N \sum_{m \in \{\text{FO,RO}\}} \frac{(J_{w,m}^{\text{exp}}(t_k) - J_{w,m}(t_k))^2}{2\lambda_{J_{w,m}}^2} \quad (3.11a)$$

$$\text{s.t. } J_{w,\text{FO}}(c_f(t), c_d(t)) = f_{w,\text{FO}}(c_f^{\text{exp}}(t), c_d(t), p), \quad (3.11b)$$

$$J_{w,\text{RO}}(c_d(t), \Delta P) = f_{w,\text{RO}}(c_d(t), \Delta P, p). \quad (3.11c)$$

To conclude, the presented approaches differ in the way of how well they can estimate the real process. White box is the simplest one where we assume theoretical equations for fluxes through both of membranes and so experimental data are not required. If the process behaves ideally, white box predicts it precisely. As we know that realistic processes do not behave this way, approaches using experimental data are required. Black box approach is more realistic as far as the flux equations are derived empirically. Empiric equations stand here for much better representation due to the fact that they include phenomena (complex interactions inside the system) which theoretical equations do not. It is still not that accurate replication of real-world phenomena, because we are not considering process dynamics and validation of material balances. We are looking only at output data values (which stand for measured flux through FO membrane) and using root mean square error minimisation technique (RMSE) we are finding model parameters which estimate these flux values as best as possible. RMSE involves minimizing the square root of the average of the squared differences between observed values and predicted ones. In the grey box approach, estimated feed concentration, feed volume, FO flux are compared with the measured values in

the loss function. Searched parameters of the FO flux model are fitted in the optimal way — which is the one in which the loss function reaches the minimal value. The main distinction between the grey and black box approaches lies in the estimation of process states through adherence to mass balance principles and their integration into the calculation of optimal model parameters. To get the better models we would need

Although the grey box approach is often considered more realistic, it does not necessarily guarantee a better RMSE evaluation for the flux variable. This is because incorporating the dynamics of the process into the model through mass balance principles reduces the degrees of freedom. As a result, this reduction can have both positive and negative impacts on the RMSE.

3.3 Process optimisation

As mentioned in the introduction (1), the purpose of modelling the processes is to understand their behaviour, anticipate process dynamics, and comprehend the relationships between inputs and outputs. For instance, in our case, we aim to understand the impact of factors such as the addition of FO/RO membranes, increasing the initial draw solution volume, and extending the running time of RO membranes. These insights gained from modelling contribute to optimisation efforts, enabling us to find the best setup based on our requirements.

The simplest approach to finding the optimal setup involves manually simulating various input and parameter combinations, and deducing the optimal setup from the simulation results. It is so called trial-and-error approach. This method does not necessitate an optimiser or a defined loss function, which simplifies its implementation. However, it also poses limitations, as we cannot be entirely certain that a better setup does not exist. This uncertainty is particularly relevant when dealing with multiple inputs whose impacts on outputs are not readily apparent.

Furthermore, for more complex tasks, such as finding a setup that achieves desired results within a specified timeframe while minimizing energy consumption, the trial and error method becomes impractical.

Our objective is to develop a program that, based on prioritization parameters (typically set by the operator or manager determining the operational strategy), identifies the optimal state by adjusting input variables to achieve the best results in the process. Subsequently, the program visualizes this optimal state, illustrating how process variables evolve over time. Additionally, it simulates the optimal solution progress,

allowing the operator to observe the simulation and verify that the given requirements are met. By prioritisation parameters we mean weighing coefficients λ_E (weight for energy), λ_t (weight for time), λ_c (weight for concentration). They are placed into the loss function as factors of the optimised variables which are: *time*, *concentration*, *energydemeand*. Time variable is a sum of partial times which represent duration of sections when RO membrane is switched off (T_1 , T_2) or switched on (T_2). Practically, these sections differ in the way of how is energy calculated. During T_1 , T_2 work of RO pump is equal to zero as the RO pump is switched off. When switched on, energy is counted via Eq. (3.9) where $dt = dT_2$. To better understand why our optimisation problem comprises precisely three sections, see the explanation bellow. We also visualise it on Figure ((3.1)). Scalar λ values allow us to designate which areas to prioritize during optimisation. A higher coefficient value signifies a greater priority in minimizing the corresponding feature. The loss function is defined as follows:

$$\min_{\Delta P, Q, T_1, T_2, T_3} \lambda_E E^N + \lambda_t \text{time} + \lambda_c (c_f^{\text{desired}} - c_f^N) \quad (3.12)$$

$$\text{s.t. } \Delta P \in (p_{\min}, p_{\max}) \quad (3.13)$$

$$\frac{dV_f(t)}{dt} = -q_{w,\text{FO}}(t) = -A_{\text{FO}} J_{w,\text{FO}}(c_f(t), c_d(t)) \quad (3.14)$$

$$\frac{dV_d(t)}{dt} = q_{w,\text{FO}}(t) - q_{w,\text{RO}}(t) = A_{\text{FO}} J_{w,\text{FO}}(c_f(t), c_d(t)) - A_{\text{RO}} J_{w,\text{RO}}(c_d(t), \Delta P) \quad (3.15)$$

$$\frac{dc_f(t)}{dt} = \frac{c_f(t)}{V_f(t)} A_{\text{FO}} J_{w,\text{FO}}(c_f(t), c_d(t)) \quad (3.16)$$

$$\frac{dc_d(t)}{dt} = \frac{c_d(t)}{V_d(t)} [A_{\text{FO}} J_{w,\text{FO}}(c_f(t), c_d(t)) - A_{\text{RO}} J_{w,\text{RO}}(c_d(t), \Delta P)] \quad (3.17)$$

$$J_{w,\text{FO}}(c_f(t), c_d(t)) = f_{w,\text{FO}}(c_f^{\text{exp}}(t), c_d(t), p) \quad (3.18)$$

$$\text{time} > 0 \quad (3.19)$$

$$\text{time} = T_1 + T_2 + T_3 \quad (3.20)$$

$$Q_f > A_{\text{FO}} J_{w,\text{RO}}(c_d(t), \Delta P) > 0 \quad (3.21)$$

Where E^N represents the sum of work done by the pump, *time* is a scalar optimised variable, c_f^{desired} is the value of the feed concentration we aim to reach, and c_f^N is the value of the feed concentration in the last step. Constraints determine the interval of acceptable pressures. p_{\min} , is set such that $J_{w,\text{RO}}(c_d(t), \Delta P)$ is always positive during the operation of the pump and smaller than the feed flow entering the pump. As we optimise FO process, its model needs to be followed (Eqs. (3.14) – (3.18)). The reason why external pressure needs to be higher than the osmotic one is because otherwise the permeate flow would reverse, which means that the draw tank would get diluted even more — the opposite effect. Flow to the RO pump must be higher than the

flow running out of it because otherwise it would not make sense. p_{\max} is the upper boundary defined by the RO membrane (the maximal pressure it can handle) or by the pump itself (the maximal pressure it can produce).

We aim to determine the minimal time required to produce the desired concentration with minimal energy input. To achieve this, we utilize the CasADi modelling language design for optimisation. It is a powerful tool capable of solving nonsigma functions and constraints (see [3]). By minimizing the loss function using this optimiser, we obtain a depiction of optimised variables (states and inputs).

In addition to optimising variables, we want the simulation to provide us with information about the running time of the RO membrane—specifically, when to switch it on and off to achieve the optimal solution based on set preferences. As partially mentioned above, to achieve this, we divide the differential equations (calculated via the Runge-Kutta method) into three sections (as depicted in the Figure (3.1), each representing a different binary scalar value indicating the state of the RO membrane (on or off). While state variables are calculated in each section, they persist for different durations of time. We have divided the process into three distinct segments because they cover all practical scenarios. We start with the system switched off, then the optimiser considers whether the RO system should be activated or remain inactive. Finally, it assesses whether the RO should be deactivated again or continue running until the process concludes. These segments encompass all relevant configurations, allowing us to focus on what we believe to be the optimal setup. While it's possible to test our hypothesis with additional sections where the RO system is periodically switched on and off, we've chosen not to include them in our analysis, focusing solely on what we consider to be the optimal configuration.

Furthermore, the simulation informs us whether we have successfully reached the desired concentration. Even when prioritizing the quality feature of achieving the desired concentration, there is only a limited concentration value that we can attain.

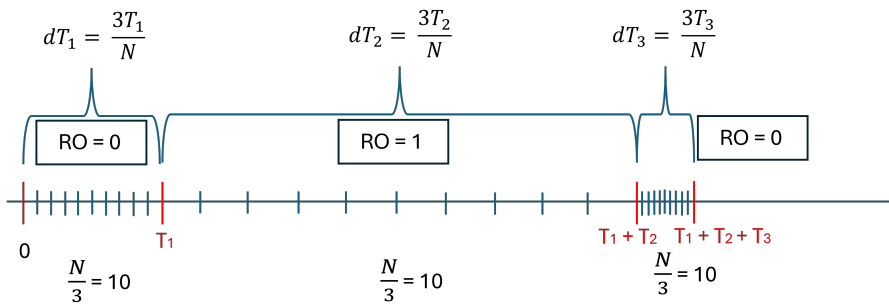


Figure 3.1: Graphical illustration of the division of time axis on three sections, each consisting of equal number of units but durates different time - dt is different for each section. First and third section are without RO impact. RO membrane is switched on from $time = T_1$ to $time = T_1 + T_2$.

Results

To find empiric models for flux through FO membrane and flux through RO membrane, experiments have been conducted to provide needed experimental data. The simulations for FO model design were gathered using a setup similar to Figure (2.1) with an FO membrane module containing hollow fibre Aquaporin FO membrane and using orange juice as the feed solution and K-lac solution. Potassium lactate solution is used as it offers high values of osmotic pressure. Its flux through RO membrane has been measured in separate experiment under constant external pressure and temperature. The temperatures of the streams were kept constant also in the FO experiment. Main difference of its experimental setup, compared to Figure (2.1), was the absence of RO membrane, thus no draw solution regeneration took place. The experiment took 4 hours and 25 minutes, after initial period with full recycle regime for the process start up and stabilisation. The starting volume in the feed tank was 250 L. The corresponding sucrose concentration of the orange juice was 11.2 Brix.

Throughout the FO module experiment run, fresh draw solution has been used and thus its concentration was kept constant. Three different concentrations were used consecutively: 20 % w/w for the first hour of the experiment, 40 % w/w in the following 84 minutes, and 60 % w/w for the rest of the experiment duration. After 45 minutes of the experiment run, feed volume was too low. Therefore, 36 L of fresh water was added over a period of 10 minutes. simulations of concentration and volume in the feed tank as well as FO membrane water flux were measured every ten seconds, yielding 1590 data points for each measured output. Volume (concentration) simulations were not recorded for one interval (two intervals) with duration of 10 minutes, which slightly reduces the dataset cardinality. The conditions of the experiment, i.e., the absence of the RO part, simplify the problem (3.10), making the Eqs. (3.1b), (3.1d) and (3.7) (and consequently Eqs. (3.10c) and (3.11c)) unnecessary.

4.1 Flux Models

Prior to using the data for model design, we have separated out the outlier points.

4.1.1 FO Model Design – White Box Approach

For the purpose of white box approach application of experimental data is not needed as the model is derived based on theoretical equations (3.6). It is not empirical.

4.1.2 FO Model Design – Black Box Approach

For the purpose of black box and grey box models data, small depiction, sample of which is shown in Table (4.1) were obtained. We have tested various polynomial models. As mentioned in the chapter above (3.2), when deciding about the mathematical structure of the model, complexity and quality of prediction are taken into account. Many of the white box approach models described in [7], which encompass processes involved in the FO process (such as concentration polarization theory, osmotic pressure models, film theory, and diffusion transport theory models), or are related to similar processes such as ultrafiltration, nanofiltration, and diafiltration—primarily exhibit polynomial structures of the first and second order, or they are logarithmic. Therefore, we have also chosen these structures for our empirical models [1].

Linear flux model has the structure: $J_{w,FO}^{estim} = a c_d + b c_f + c$. Coefficients a, b, c where obtained by minimisation of RMSE between estimated flux values and measured ones. Following linear equation has been derived:

$$J_{w,FO}^{estim}(c_d, c_f) = 0.0922c_d - 0.248c_f + 9.64 \quad (4.1)$$

Quadratic flux model has the structure: $J_{w,FO}^{estim} = a c_d + b c_d^2 + c c_f + d c_f^2 + e$. Similarly as for the linear model, all of the coefficients where obtained by minimisation of RMSE between estimated flux values and measured fluxes. Following quadratic equation has been derived:

$$J_{w,FO}^{estim}(c_d, c_f) = 0.345c_d - 0.00296c_d^2 - 0.455c_f + 0.00250c_f^2 + 8.67 \quad (4.2)$$

When deciding about the structure of model including logarithmic function we took the inspiration from film theory for ultrafiltration process [1]. The flux equation here has the form:

$$J_w(c_f) = \frac{D}{\delta} \ln \frac{c_w}{c_f} \quad (4.3)$$

where $\frac{D}{\delta}$ is a mass transfer coefficients, typically denoted k , c_w stands for "wall concentration" which is the maximal solute concentration and it occurs in the close distance from membrane. c is bulk concentration, which is the lowest feed concentration. Because of this fact there comes to membrane polarisation, consequence of which is back diffusion [1].

We have implemented this equation in the following form:

$$J_{w,FO}^{\text{estim}}(c_f) = k \ln \frac{c_{lim}}{c_f} = k(\ln c_{lim} - \ln) c_f = b - ax \quad (4.4)$$

k is a constant, c_{lim} represents maximal feed concentration for which we get non-zero flux. It is determined by the value of draw concentration. The higher is a draw solution's concentration the higher is also c_{lim} value. We can find it via linear regression when transforming the equation into the linear form (4.4). c_f serves as an independent variable. Employing the black box modelling approach, we have found two models for two values of draw concentration: 20% and 40%. Unfortunately, flux data obtained for a draw concentration of 60% exhibited significant deviation, leading to the exclusion of these data points from the model fitting process due to their large standard deviation.

For the draw concentration of 20% we got equation:

$$J_{w,FO}^{\text{estim}}(c_f) = 25.5 + 6.5 \ln c_f = 6.5 \ln \frac{50.6}{c_f} \quad (4.5)$$

and for draw solution of 40%:

$$J_{w,FO}^{\text{estim}}(c_f) = 50.19 + 12.57 \ln c_f = 12.57 \ln \frac{54.25}{c_f} \quad (4.6)$$

To derive the general model where the parameter c_d is introduced as a second independent variable, we have to extrapolate from these two univariate models, noting the linear relationship between the intercept and slope with respect to c_d . Using c_d , we can express the intercept as: intercept = $\frac{c_d}{20} \times 25.5$, and similarly for the slope: slope = $\frac{c_d}{20} \times (-6.5)$. This results in the model:

$$J_{w,FO}^{\text{estim}}(c_f, c_d) = \frac{c_d}{20} (25.5 - 6.5 \ln c_f) \quad (4.7)$$

The issue arises from the fact that the model was derived solely from two values of draw concentration (20% and 40%), which means it should not be applied to different concentration ranges. However, data obtained for a draw concentration = 60% was imprecise, of high variation, it has contributed to the design of linear and quadratic model models. That is why we can apply them also for ranges 40 – 60%.

c_d [%]	c_d^2 [% ²]	c_f [Brix]	c_f^2 [Brix ²]	$J_{w,FO}^{\text{measured}}$, [LMH]
20	400	11.2	125.44	9.89
20	400	12.35	152.45	9.15
40	1600	37.25	1387.78	4.38
40	1600	38.73	1500.3	3.62
60	3600	53.98	2914.03	1.18
60	3600	56.09	3145.96	1.18

Table 4.1: Measured data for models design using black box approach

$J_{w,FO}^{\text{estim, linear}}$	$J_{w,FO}^{\text{estim, quadratic}}$	$J_{w,FO}^{\text{estim, log (20% - 40%)}}$	$J_{w,FO}^{\text{estim, log (20% - 60%)}}$
9.53	8.71	9.8	8.88
9.09	8.42	9.17	8.34
4.08	4.25	3.99	5.037
3.71	3.86	3.48	4.6
1.43	1.77	-1.2	1.69
1.07	1.25	-2.0	1.05

Table 4.2: Estimation of water flux in LMH units using black box approach for linear, quadratic and logarithmic models

To get a logarithmic model which is applicable in wider concentration scale we need to change its structure. When finding such model we must adhere to the principles of the black box approach, reformulate the structure of the the model into linear form and determine its coefficients. Following this approach, we have derived:

$$J_{w,FO}^{\text{estim}}(c_f) = ac_d + bc_d \ln c_f = 1.15c_d - 0.2778c_d \ln c_f - 0.62541 \quad (4.8)$$

When compared with the equation (4.5) by substituting c_d for 20 we get equation:

$$J_{w,FO}^{\text{estim}}(c_f) = 22.93 - 5.4 \ln c_f - 0.6254 \quad (4.9)$$

which is similar to (4.5). However, (4.8) is derived from a more varied set of experimental data, including $c_d = 60\%$. Consequently, this model can be applied to cases where c_d exceeds 40%. However, it is less accurate for draw concentrations ranging from 20 to 40 mass percent compared to (4.7)

The columns of Table (4.2) represent estimated flux values calculated using derived models. The quality of prediction is evaluated using RMSE criteria displayed in charts. Models achieving lower RMSE values are considered more appropriate. On first glance,

	Coefficient	Standard Error	t-stat	p-value	↓ 95%	↑ 95%
Interc.	8.67	0.138	62.78	0	8.40	8.94
c_d	0.345	0.0085	39.48	0	0.333	0.368
c_d^2	-0.00296	1.1×10^{-4}	-25.9	0	-0.0027	0.0032
c_f	-0.455	0.00849	-53.59	0	-0.47	-0.44
c_f^2	0.0025	1.1×10^{-4}	23.5	0	0.0023	0.0027

Table 4.3: Output from data analysis solver providing essential information about the model coefficients

we can conclude that the logarithmic model 20% - 40% (4.7) estimates flux values very well for lower feed concentrations and adequately for the higher ones (this is related to the training dataset from which it was derived, as discussed above). On the other hand, the logarithmic model 20% - 60% predicts flux values for higher concentrations (both draw and feed) better but performs worse for lower concentrations. More detailed discussion of these results is provided below.

To evaluate the quality and characteristics of the calculated parameters, tables displaying essential statistical information about the model coefficients have been generated. These tables were computed for each model designed using the black box approach. We will analyze these tables in detail, with a particular focus on the one that describes the coefficients of the quadratic model, as it has the most estimated parameters. The table in question is displayed in Table 4.3.

The second column in the Table (4.3) is of particular importance as it contains the identified coefficient values, which are the focus of our analysis. Further interpretation of these coefficients is provided below.

The third column of the Table (4.3) represents standard error values, which provide a measure of the variability of the estimated coefficients. A smaller standard error indicates a more precise estimate of the coefficient value displayed in the first row of the Table (4.3).

In the fourth column, t-statistic values are displayed, calculated as the division of coefficients by their standard error values. A larger absolute value of the t-statistic suggests that the coefficient is statistically more significant and is used for constructing confidence intervals, displayed in the sixth and seventh columns of the Table (4.3). In more detail they are explained below.

The fifth column contains p-values, which represent the probability of rejecting the null hypothesis (that the corresponding coefficient is equal to zero). A low p-value (typically less than 0.05) indicates a small probability and suggests that the variable is statistically significant and should not be excluded to avoid multicollinearity. However, coefficients in front of variables raised to the second power are close to zero; their low p-values indicate significance. The reason for these low coefficients is that the change in the variable becomes more pronounced when it is squared, necessitating compensation by these lower coefficients.

The sixth and seventh columns provide the estimated range of values within which a true population parameter is likely to fall with a 95% level of confidence. A smaller range indicates higher precision. It is important for the interval not to contain zero. Otherwise, it suggests that the coefficient could be zero, indicating that the variable is not statistically significant and should be excluded from the model. For this reason we exclude variable c_d^2 from our model as its interval contains zero. Subsequently we retrain the model to get more accurate values for model parameters.

Based on theoretical knowledge, we expect that water flux values should increase with the rise of draw concentration due to a higher driving force, while flux values decrease with increasing feed concentration as the osmotic pressure difference between draw and feed solutions diminishes, resulting in a lower driving force. This trend is confirmed by both linear and quadratic models. However, the coefficients in front of quadratic independent variables have mutually opposite signs. Nonetheless, the overall trend is preserved, as these quadratic variables contribute to a convex characteristic of the draw concentration variable and a concave characteristic of the feed concentration variable. To better understand the impact of each independent variable on flux value, we have plotted charts (Figures (4.2), (4.1)) showing the relationships between the output and each separate independent variable.

We observe that the trend of $J_{w,FO}$ with respect to c_d increases only up to approximately 60% draw concentration. This is attributed to imprecise and noisy data with high variance obtained for higher concentrations of feed and draw solutions. Similarly, in chart 4.2, the change in trend (from decreasing to rising) occurs later, at 90 brix. These observations suggest that the model should be used only for draw solution concentrations smaller than 60%.

Results interpretation

To see the accuracy of the models of flux prediction, charts depicting dependencies of fluxes (measured and estimated) have been plotted: Figures (4.3), (4.4), (4.5)

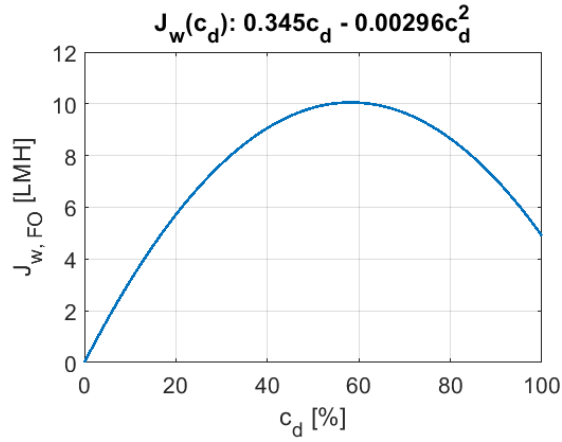


Figure 4.1: Impact of draw solution on flux in quadratic FO model designed applying black box approach.

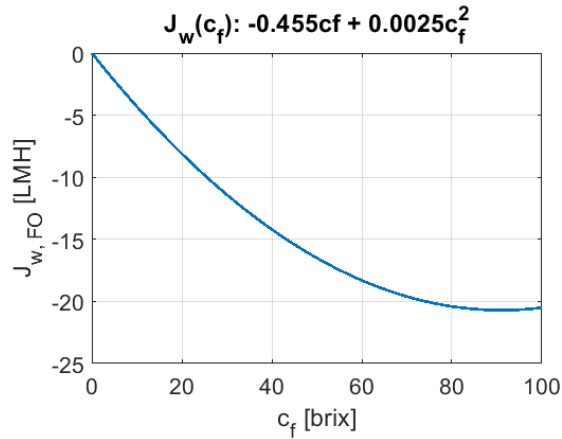


Figure 4.2: Impact of feed solution on flux in quadratic FO model designed applying black box approach.

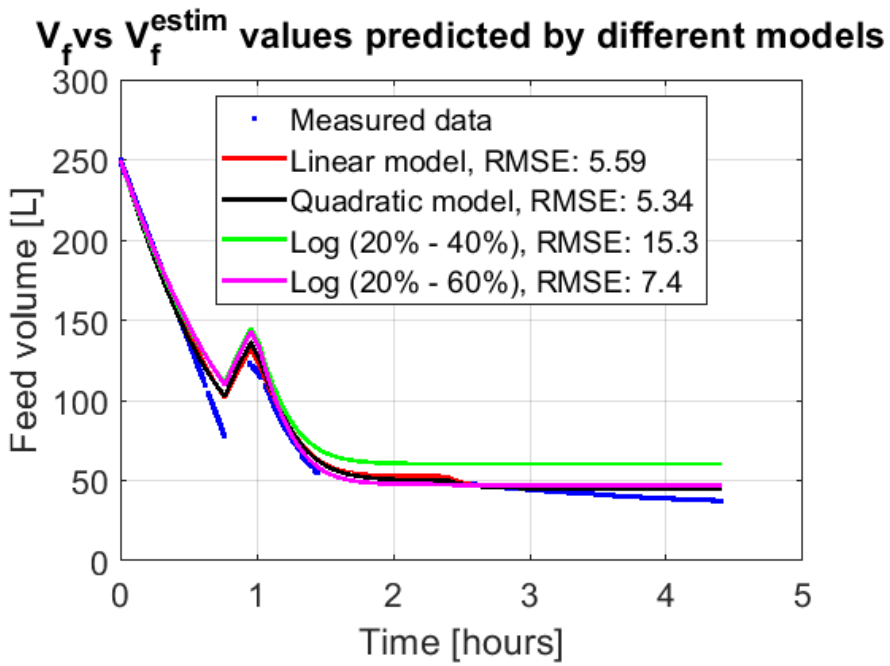


Figure 4.3: Model response while fitting the evolution of feed volume in time using various fitting models - black box approach.

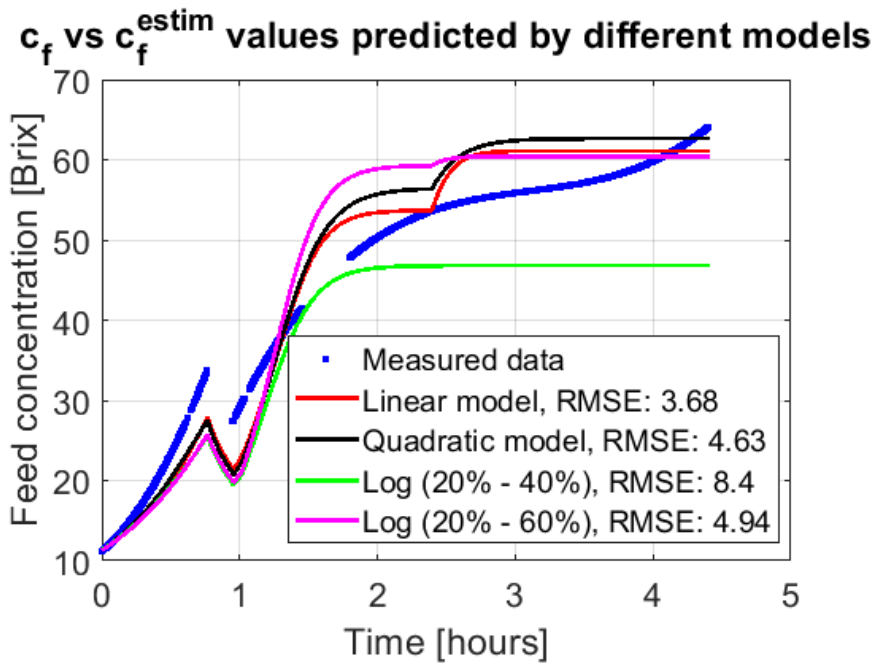


Figure 4.4: Model response while fitting the evolution of feed concentration in time using various fitting models - black box approach.

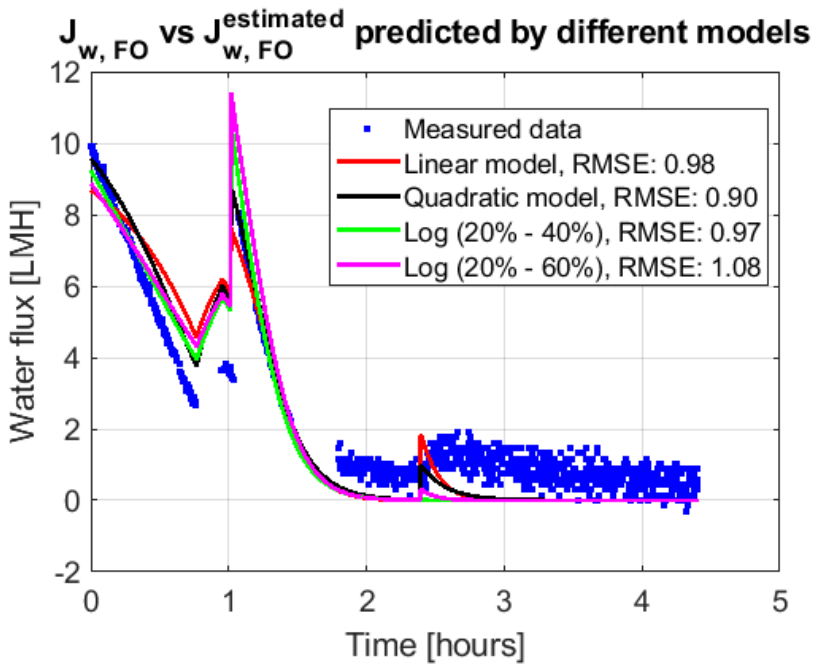


Figure 4.5: Model response while fitting the evolution of water flux in time using various fitting models - black box approach.

Based on the depicted charts (Figures (4.3), (4.4), (4.5)), we can conclude that all of the models aim to capture the trend of measured states, although some more accurately than others. The evaluation of each model has been conducted using the RMSE method, with the dataset divided into 80% training data and 20% testing data. The training dataset has been utilized for model development (training), while the testing data has been used to assess the model's quality (validation). Each model exhibits different sensitivity, reacting uniquely to changes in draw concentration.

The quadratic model yields the lowest values for flux and volume variables. For feed concentration prediction, the linear model seems to be the most suitable. Therefore, we can consider these two models as the most appropriate ones. The choice between them depends on which variable is more crucial for prediction. If concentration is prioritised, the linear model is preferable, while for flux or volume, the quadratic model should be chosen. This prioritisation of state variable prediction is one of the benefits of the grey box approach.

The logarithmic model (20-40%) confirms its validity only within this concentration range, as the increase in draw solution from 40% to 60% does not exhibit a clear trend. This is because the data for draw solution 60% were excluded from the model training process. Based on its RMSE values for all observed state variables, we can identify this model as the least accurate among the four selected models, although it does not provide the highest RMSE values for flux.

The logarithmic model (20-60%) achieves overall lower RMSE values as a consequence of including 60% c_d values. However, compared to the linear and quadratic models, it is less accurate.

All models provide inaccurate estimates for higher concentrations (at later times) due to imprecise measured data during this period. To enhance model accuracy, simulations for a wider range of draw concentration values should be conducted. Currently, there are only three values – 20, 40 and 60%.

4.1.3 FO Model Design – Grey Box Approach

By solving the optimisation problem (3.10) Using the casADi language designed for optimisation in the Python environment, we have developed linear and quadratic models to estimate the FO process. Minimising the RMSE of not only the flux variable but also the feed volume and concentration has advantages, as we can prioritise which state to focus on more using scalar λ values. These λ values represent the standard deviation, which is related to the precision of their capture during the experiment. For

example, if the volume can be measured with higher accuracy, this state variable has a lower standard deviation and is therefore prioritised more. Lower λ values in the denominator cause a higher weight on the given state variable. Since the experiment was conducted only once and the states do not attain a steady state, we do not know the value of the standard deviation. We can only estimate it based on how the states were measured, which of them were likely to reach higher variance. This fact can be further refined when repeating the experiment more times, however, at present, it is not that important. To demonstrate the influence of λ values, we plot scenarios with four different λ values for linear, quadratic, and logarithmic models. The logarithmic model in the form of (4.5) has not been designed by the grey box model, as the casADi encountered difficulties in establishing parameters for this structure of the model.

Mathematical models for each model structure and unit λ values:

$$J_{w,FO}(c_d, c_f) = 0.089c_d - 0.26c_f + 10.49 \quad (4.10)$$

Linear model – comparison with other approaches :

- grey box (GB): $J_{w,FO}(c_d, c_f) = 0.089c_d - 0.26c_f + 10.49$
- black box (4.1) (BB): $J_{w,FO}(c_d, c_f) = 0.092c_d - 0.248c_f + 9.6412$
- white box (WB): Osmotic pressure of feed and draw have been determined empirically and substituted into WB FO model Eq. (3.6) and applying empiric model for osmotic pressure of draw solution (Eq. (3.8)) and model for osmotic pressure of feed: $\Pi_f = 0.0103c_f^2 + 0.9423c_f + 3.27$ we get WB model: $0.55((0.2267c_d^2 - 0.835c_d) - (0.0103c_f^2 + 0.9423c_f + 3.27))$. When substituting for c_d 20% and for c_f 11.2 Brix we get flux value of 32LMH which is compared to GB which reaches for the same values of c_f and c_d flux = 9.4LMH. Using BB is the flux value = 8.7LMH. We can see that WB does not provide accurate prediction.

$$J_{w,FO}(c_d, c_f) = 0.0743c_f^2 - 0.131c_d - 0.414c_f + 7.01 \quad (4.11)$$

Quadratic model: comparison with other approaches:

- GB: $J_{w,FO}(c_d, c_f) = 0.0743c_f^2 - 0.131c_d - 0.414c_f + 7.01$
- BB: (Eq. (4.2)) $J_{w,FO}(c_d, c_f) = 0.0025c_f^2 + 0.345c_d - 0.45524c_f + 8.67$

- WB: As there is only one form of White box approach model, it provides the same result as above – in linear model comparison (4.1.3).

For $c_d = 20\%$ and $c_f = 11.2\text{Brix}$ we get for GB: 9.1LMH For BB: 10.8LMH

$$J_{w,\text{FO}}(c_d, c_f) = 1.46c_d - c_d \ln(c_f) 0.348 - 1.9 \quad (4.12)$$

Logarithmic model (20% – 60%): comparison with other approaches:

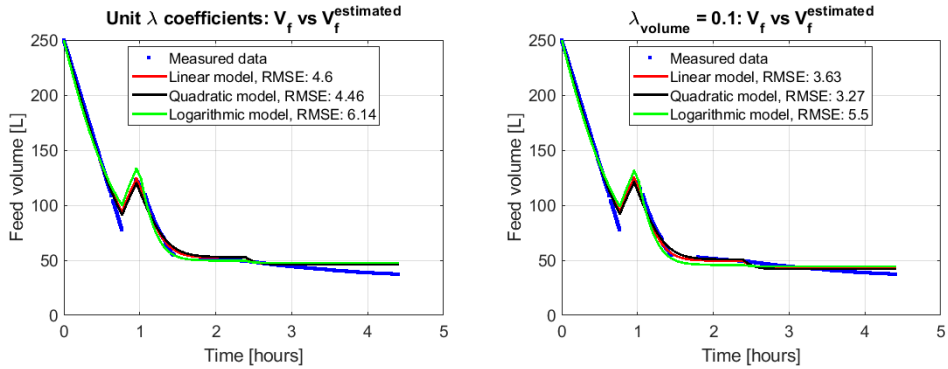
- GB: $J_{w,\text{FO}}(c_d, c_f) = 1.46c_d - 0.348c_d \ln(c_f) - 1.9$, which is for above stated c_f and c_d values = 10.5LMH.
- BB: (Eq. (4.4)) $J_{w,\text{FO}}(c_d, c_f) = 1.15c_d - 0.2778c_d \ln(c_f) - 0.63$, which is for above stated c_f and c_d values = 8.96LMH.

As observed from the comparison between the black box and grey box (4.1.3) approaches, these methods yield similar outcomes. However, it's crucial to note that they were only tested with a single value for c_d and c_f , making the validation less robust. To address this, we present graphical comparisons in the figures below. Figures (4.6a) – (4.8d) show the influence of λ parameter on estimated process variables. Figures (4.9a) – (4.11c) illustrate the comparison between BB and GB models to provide a more comprehensive validation than the single-value approach previously employed.

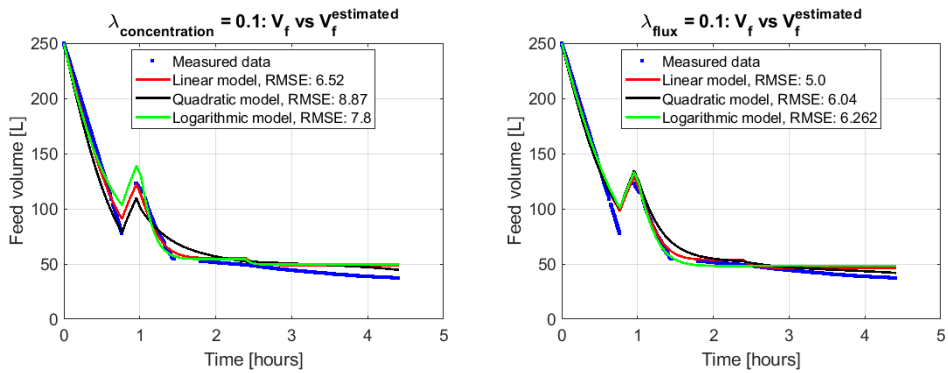
Results interpretation

Based on the plotted charts (Figures (4.6a) – (4.8d)) and RMSE values we can declare the correctness of the hypothesis that λ values can be used as prioritising parameters. When applying a lower λ value (causing the higher weight of the given variable in the loss function), the model predicts the variable more accurately (resulting in a lower RMSE value).

Valuable information worth noting is that the quadratic fit consistently achieves lowest RMSE values compared to other models when the priority is set on the λ for the currently observed variable. For example most accurate model for V_f , when the λ parameter with the lowest value is λ_{V_f} is quadratic model. The same way it works also for other estimated variables. This may be attributed to the fact that the quadratic model has more coefficients, allowing it to better adapt to the set criteria compared to simpler models with fewer optimised parameters. Thus, it is more sensitive. Conversely,

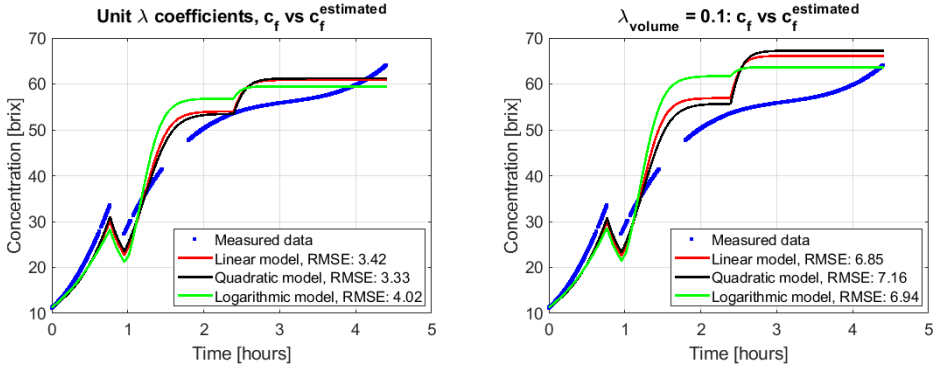


(a) Grey box models response – V_f estimation for unit λ values (b) Grey box models response – V_f estimation for ten times lower λ_V value

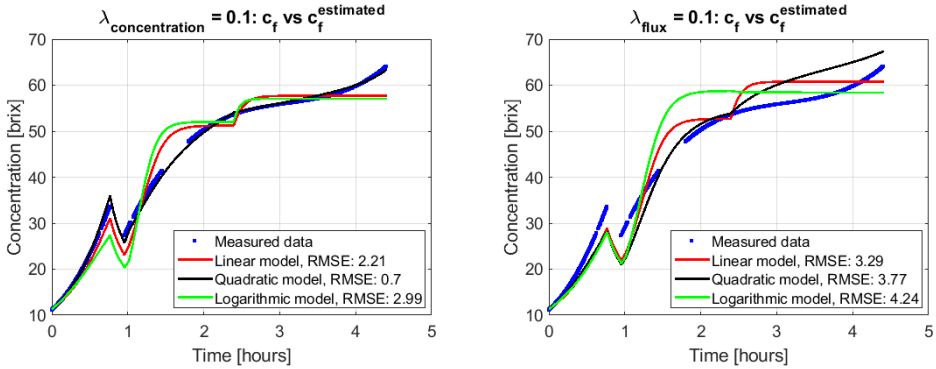


(c) Grey box models response – V_f estimation for ten times lower λ_c value (d) Grey box models response – V_f estimation for ten times lower λ_{flux} value

Figure 4.6: Comparison of measured and estimated data for feed volume by grey box approach for different values of standard deviations.

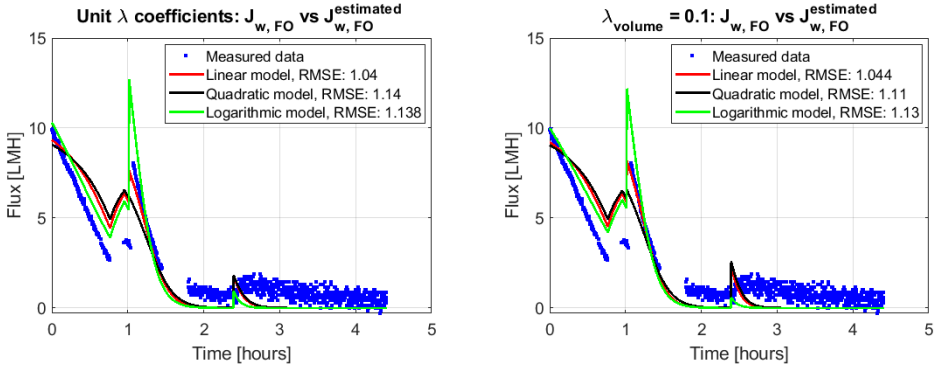


(a) Grey box models response – c_f estimation for unit λ values (b) Grey box models response – c_f estimation for ten times lower λ_V value

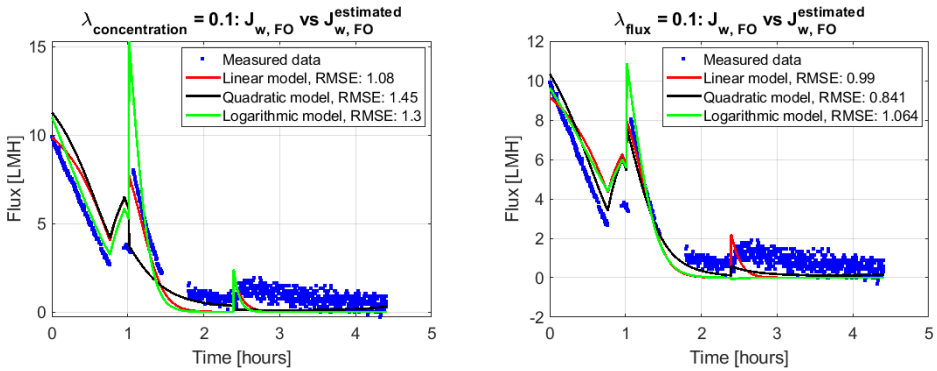


(c) Grey box models response – c_f estimation for ten times lower λ_c value (d) Grey box models response – c_f estimation for ten times lower λ_{flux} value

Figure 4.7: Comparison of measured and estimated data for feed concentration by grey box approach for different values of standard deviations.



(a) Grey box models response – $J_{w,FO}$ estimation for unit λ values (b) Grey box models response – $J_{w,FO}$ estimation for ten times lower λ_V value



(c) Grey box models response – $J_{w,FO}$ estimation for ten times lower λ_c value (d) Grey box models response – $J_{w,FO}$ estimation for ten times lower λ_{flux} value

Figure 4.8: Comparison of measured and estimated data for flux by grey box approach for different values of standard deviations.

when the priority is on another state variable that is not visualised, the RMSE is higher. So we can say that quadratic model is adaptable in bigger extent than linear or logarithmic models. Sense of λ parameters is in the possibility to focus on selected state during the model design. By changing the λ value model changes as well. If the primary objective is to achieve the most accurate prediction of flux, while other process variables are of lesser importance, reducing the value of λ_{flux} results in a model that predicts flux more precisely (with potentially less accuracy for feed concentration and feed volume). According to RMSE validation, the linear and quadratic models offer the best estimations.

Similarly as it was for black box approach, logarithmic model 20% – 60% reaches overall higher RMSE values what makes less appropriate model out of it.

4.1.4 Grey box vs Black box results comparison

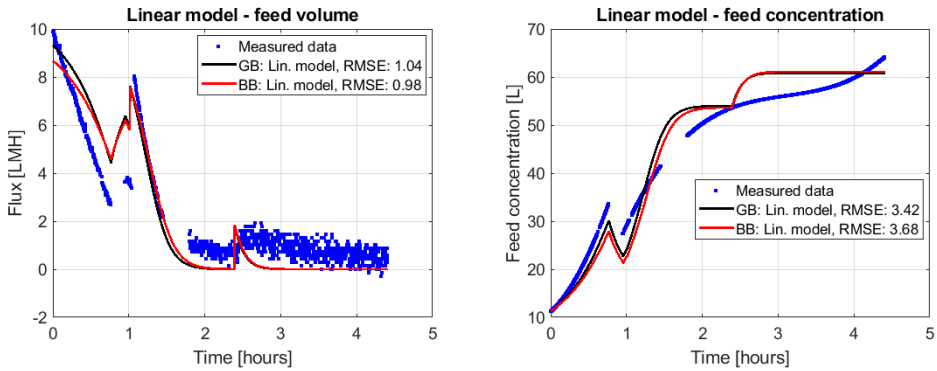
To better understand which modelling approach yields better results, grey box charts for unit λ parameters were plotted and compared with charts capturing black box models. The results can be seen in Figures (4.9a) – (4.11c).

Results interpretation

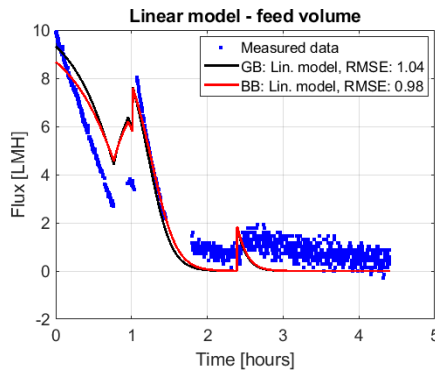
Based on the plotted charts (Figures (4.9a) – (4.11c)), we can conclude that models designed using the grey box approach better capture the process states. This is because the grey box approach, unlike the black box approach, follows mass balances. However, flux is estimated with higher precision by the black box approach, as it is the only variable occurring in the loss function. This better prediction is attributed to the fact that the black box approach can minimise the error between measured and estimated flux without the states adhering to mass balance laws, providing greater freedom and a smaller number of optimised variables. Given these considerations, alongside the observation that the linear model developed through the grey box approach averagely yields the lowest RMSE values, our subsequent efforts in process optimisation will primarily leverage this particular model.

4.2 Model Validation

Based on the experimental data, we can conclude that higher the feed concentration, higher the flux simulations variate. We thus cannot expect any of the trained models to be particularly suitable for accurate prediction in such conditions. From the fitting

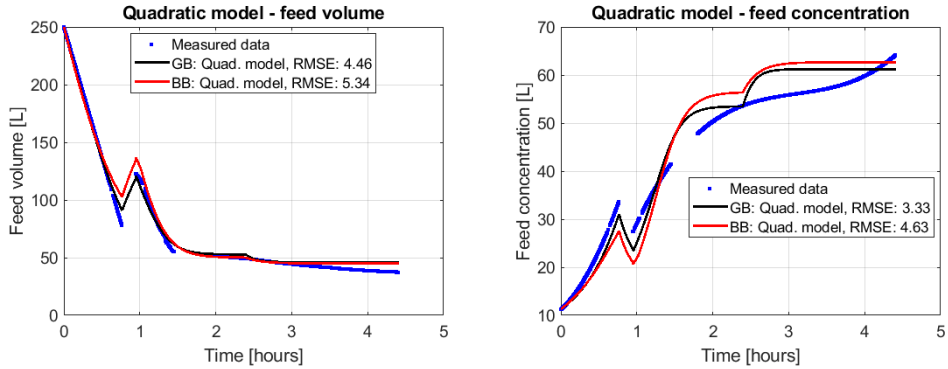


(a) GB vs BB, linear model – V_f estimation for unit λ (b) GB vs BB, linear model – c_f estimation for unit λ

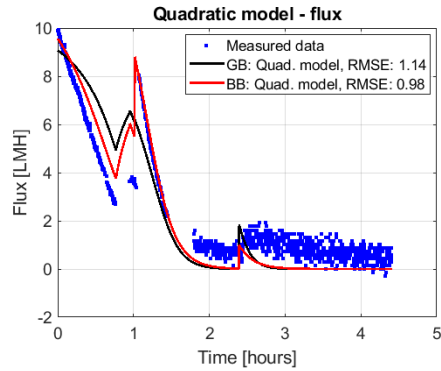


(c) GB vs BB, linear models – $J_{w,FO}$ estimation for unit λ

Figure 4.9: Comparison of measured and estimated process states by linear model derived from two different modelling approaches: GB and BB.

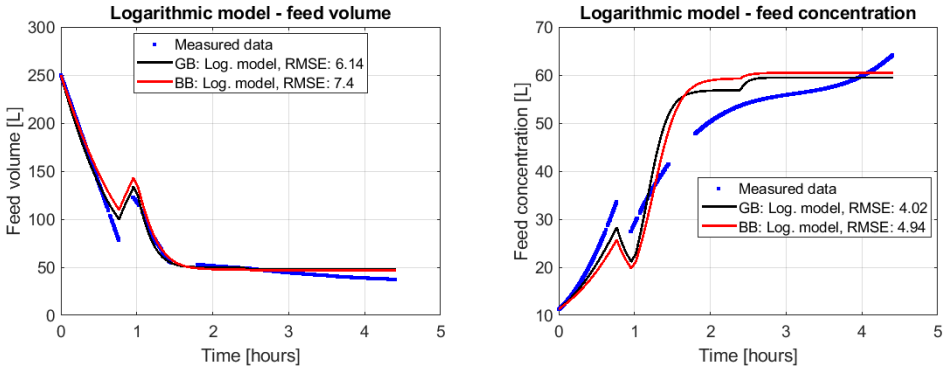


(a) GB vs BB, quadratic model – V_f estimation for unit λ values (b) GB vs BB, quadratic model – c_f estimation for unit λ

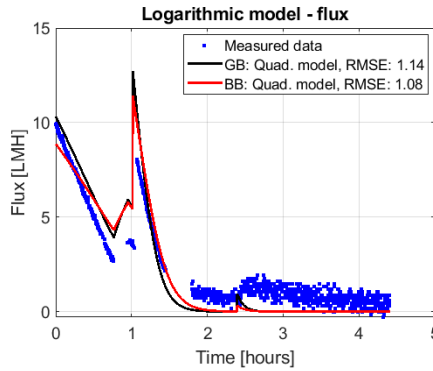


(c) GB vs BB, quadratic model – $J_{w,FO}$ estimation for unit λ

Figure 4.10: Comparison of measured and estimated process states by quadratic model derived from two different modelling approaches: GB and BB.



(a) GB vs BB, logarithmic model – V_f estimation for unit λ (b) GB vs BB, logarithmic model – c_f estimation for unit λ



(c) GB vs BB, logarithmic model – $J_{w,FO}$ estimation for unit λ

Figure 4.11: Comparison of measured and estimated process states by logarithmic model derived from two different modelling approaches: GB and BB.

results of all depicted charts (Figures (4.3) – (4.11c)) it is apparent that the fit is best for the data in the first hour of the experiment with low concentrations of feed and draw solutions. The fit gets evidently worse already for the values $c_d = 40\%w/w$. For the last part of the experiment (with high feed concentrations), one cannot reliably conclude appropriateness of the fit. Looking at for example Figure (4.11c), one can observe that the model performs even worse and if used for further purpose, e.g., process design or optimisation, its results would be unsatisfactorily when compared with reality.

When fitting the grey box models, the best form of the flux equation, (Eq. (3.10b)) turned out to be quadratic and linear, which shows a similar trend as the black box models (Figures (4.9a) – (4.11c)). As far as the accuracy of both models is very similar the simpler one is preferred. At this point, we can also assess the appropriateness of the white box model. If the white box model was appropriate, i.e., if the FO flux can be described by Eqs. (3.8) and (3.6), the grey box model would turn out to contain similar coefficients multiplying feed and draw concentrations. As we can see from (4.1.3) this is not the case that we observe here. White box does not provide correct results in other case. It serves mainly as a base for GB and BB approach development. We thus conclude that the white box model is unsuitable in this application.

4.3 RO Flux Model Derivation

Finding of model for flux through RO membrane is easier problem than doing so for FO, because the model is univariate - only the draw concentration is considered as an independent process variable (its osmotic pressure respectively (3.8)). The other variables influencing the flux (pressure, temperature) were held at constant values. Osmotic pressure was calculated using white box logarithmic model (3.8). Relation between osmotic pressure of draw solution (K-lac) and its concentration is known due to conducted experiment (shown in Figures (4.12a), (4.12b)). By plotting the relation between measured flux and concentration/osmotic pressure we can simply derive the model.

By conducting linear regression analysis on the data depicted in Figure (4.12b), we established the RO model represented by the linear equation (Eq. (4.13)). With a root mean square error of 0.949, the model demonstrates a strong fit to the data. The negative slope of the linear coefficient signifies that higher draw concentrations necessitate increased external pressure to counteract the rising osmotic pressure. Notably, the highest flux occurs at a draw concentration of zero, equivalent to the intercept of 20.66LMH. This model is applicable in scenarios where a constant pressure

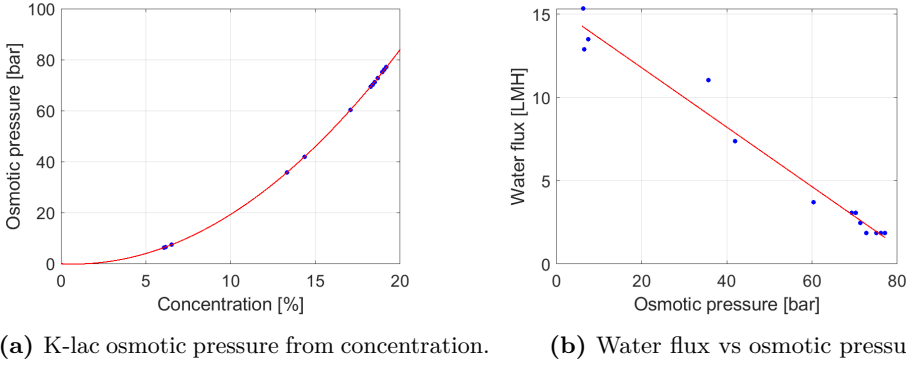


Figure 4.12: Results from RO flux experiment

of approximately 100 bar is maintained.

$$J_{w,RO} = -1.11c_d + 20.66 \quad (4.13)$$

4.4 Process Optimisation

As outlined in the theoretical section (3.3), our secondary objective was to optimise the FO process using the developed models. Our optimisation efforts primarily focus on improving temporal efficiency, minimising energy consumption, and achieving desired quality levels in the process. To attain these objectives, we employ various weighting coefficients to prioritise specific optimisation targets. Higher weight coefficients indicate a greater emphasis on optimising the associated variable. For instance, to prioritise energy minimisation over process duration, we initially assign a significantly higher value to the λ_E parameter compared to λ_t , and iteratively adjust these parameters until the desired optimisation outcome is achieved. Similarly, by adjusting the λ_t parameter, we can alter the priority given to process duration. These λ values serve as tuning parameters, allowing us to fine-tune the optimisation process.

To explore the influence of λ values on process dynamics and optimal input configurations, we conducted simulations as outlined in the Table (4.4). These simulations encompassed various process characteristics, including the temporal evolution of state variables (V_f , V_d , c_f , c_d , Φ_d , W), flow rates through FO and RO membranes (Q_{FO} , Q_{RO} , both in L/h), input variables such as draw solution flow rate to the pump

($Q_{\text{pump}}[L/h]$), and external pressure ($\Delta P[\text{bar}]$). Additionally, we recorded optimised variables such as the duration of RO operation ($t_2[\text{h}]$), the duration of RO activation and deactivation (t_1 and t_3 , respectively, both in $[\text{h}]$), total energy consumption $E_{\text{sum}}[\text{bar}\frac{\text{L}}{\text{h}}]$, and the final feed concentration ($c_{\text{fin}}\text{Brix}$). Duration of the process ($\text{time}[\text{h}]$) is sum of t_1 , t_2 and t_3 . Values of these optimised variables for various λ coefficients are shown in Table (4.4). Each characteristic was simulated across 10 iterations, with each iteration representing a unique combination of standard deviations of optimised variables.

Constant process parameters included an FO membrane area of 2 m^2 , an RO membrane area of 0.7 m^2 . Such parameters were chosen for the first set of simulations because of the fact that same ones were used also in FO and RO experiments which we discussed above. The desired feed concentration was set to 30 Brix from an initial concentration of 11.2 Brix. The initial concentration of the draw solution was $c_{d0} = 26.4$ Brix, and the initial tank volumes were set to 250L. The same draw and feed solutions were naturally used as in the modelling experiments. For FO flux prediction, we used a linear model derived using the grey box approach, as explained in section (4.1.4).

The program was developed in casADi within a Python environment, similar to the grey box model. It includes the definition of optimised variables and process functions, which enter differential equations for state variables and their dynamic representation and calculation using the Runge-Kutta method. Optimisation is performed via loss function and constraints definitions (both shown in Eq. (3.21)).

	λ_E	λ_t	λ_c	t_1	t_2	t_3	time	c_{fin}	E_{sum}
1	3.1×10^{-5}	1	1	5.5	0	5.2	10.7	29.8	0
2	2.9×10^{-5}	1	1	0	7.1	2.7	9.76	29.8	18410
3	2.3×10^{-5}	1	1	0	7.64	2.08	9.73	29.8	19622
4	1.3×10^{-5}	1	1	0	8.5	1.2	9.7	29.8	21235
5	1	1.0×10^6	1.0×10^5	0.1	8.9	0.3	9.3	28.4	21255
6	1	1.0×10^6	1.0×10^4	0	0	0	0	11.2	0
7	1	1.0×10^5	1.0×10^5	0	9.3	0.37	9.7	29.8	22653
8	1	1.0×10^4	1.0×10^5	5.5	0	5.3	10.8	30	0
9	1	2.5×10^4	1.0×10^5	0	5.82	4.07	9.89	30	15655

Table 4.4: Table of values of optimised process variables dependent from λ parameters

The significance of λ values lies in their role in prioritising the minimisation of specific optimised variables. Properly setting these values allows us to effectively achieve our optimisation goals. Essentially, λ values serve as a form of economic expression, where

a higher λ value indicates a higher priority for minimising the associated variable. While λ values can be interpreted in an economic context, it's important to note that our focus in this work is not on the economic aspect, and therefore we won't delve into that aspect. As mentioned, determining what constitutes a high λ value is specific to each optimisation scenario and requires experimental determination through trials.

In the first simulation (first row in Table (4.4)), energy is prioritised as the RO membrane is not switched on at all, resulting in zero energy consumption by the pump. The evolution of states is depicted in the Figures (4.13) – (4.16). Feed concentration rises until it reaches the desired level, while draw concentration decreases due to lack of regeneration. Similarly, feed volume decreases as it is a batch process, while the draw tank volume increases. Flux through FO decreases with the lower concentration of draw solution and higher feed solution.

In the third and fourth simulations, we continuously lowered λ_E to observe if our hypothesis that lowering it would result in reaching the desired concentration more quickly, albeit with a higher energy load, was correct (see the Table (4.4), 3rd and 4th rows). Subsequently, we fixed the value for λ_E to a constant unit value for all following cases and started to change the other two λ values to observe the consequences. The sixth case serves as an example of what happens when λ values are set inappropriately. Due to the fact that the reach of the desired concentration is significantly lower compared to the fifth row (where the RO membrane was switched on for almost the entire duration as a consequence of high λt), time and energy prioritisation are too high compared to concentration priority, resulting in the process stopping immediately.

The combination of $\lambda t = 2.5 \times 10^4$ and $\lambda c = 1 \times 10^5$ reduces to the first case where the RO has not been switched on.

The last combination of coefficients represents a scenario in which the membrane is switched off first and then turned off again. The reason for this behaviour is that the forward osmosis (FO) flow is highest for lower feed concentrations and regenerated draw concentration. At higher feed concentrations, the impact of using regenerated draw solution compared to not regenerated is not as significantly reflected in FO flux values as it is for lower feed concentrations. Conversely, when the goal is to minimise energy consumption as much as possible, it is more efficient to run the reverse osmosis (RO) later, as lower draw concentration occurs in the tank. This represents a lower external pressure necessary to be applied, resulting in lower overall energy consumption.

As we can see, majority of cases follow the same trend. The membrane is first switched on and then, depending on the particular λ values, switches off. Conversely, this

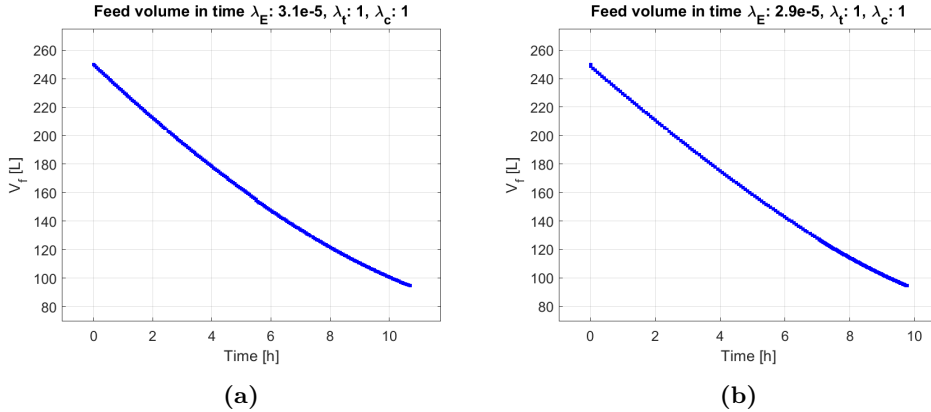


Figure 4.13: Feed volume in time: In second scenario it decreases slower because of lower driving force – osmotic pressure of draw solution

doesn't occur as frequently. We will test this further in the following experiment.

Quickest time to reach the desired concentration was the fifth case ($time = 9.3h$). It was the fastest case because the RO was switched on for almost the whole overall running time (except 0.4h). The other thing is that $c_{f,desired}$ was not reached completely (final value was 28.4 Brix). To get the higher value – closer to $c_{f,desired}$ we need to higher the λ_c value. Such case is the 7th one. Here desired value is reached in 9.7h while consuming more energy.

To see the impact of λ values on other process features, charts for the first-row scenario (no influence from RO as it is switched off) and second-row scenario have been depicted, showing time dependencies for states and input variables.

When adjusting the λ values according to the manual, we start with a higher λ_E and gradually decrease it until we achieve the desired result. If the result is not satisfactory, we proceed to adjust the coefficients further. To enable the RO pump to switch on, λ_E needs to be lowered, or alternatively, λ_c increased (as seen, for example, in cases 5 and 6 in Table (4.4)). A decrease to 2.9×10^{-5} caused the RO to switch on, remaining on for around seven hours before being switched off for approximately three hours. The impact of this switch is shown in a shorter time frame but at the expense of an energy consumption equal to $18410 \text{bar} \frac{\text{L}}{\text{h}}$. The evolution of RO flow and energy of the second tested case are depicted in the Figures (4.19b), (4.17b), along with the impact of the RO on c_d (Figure (4.16b)) when compared with scenario with no impact of RO (first

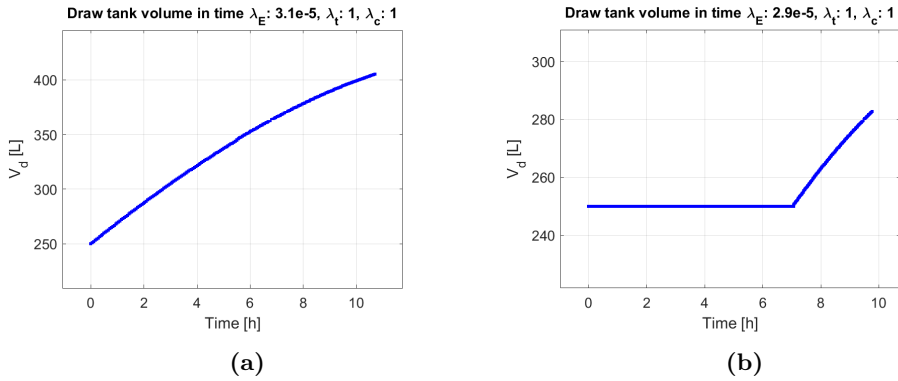


Figure 4.14: Volume of draw tank: In the first case, it spontaneously increases because of FO flux which flows into it from the feed tank. In the second one, it remains at the lowest possible level (representing maximal concentration) until the seventh hour when RO is switched off.

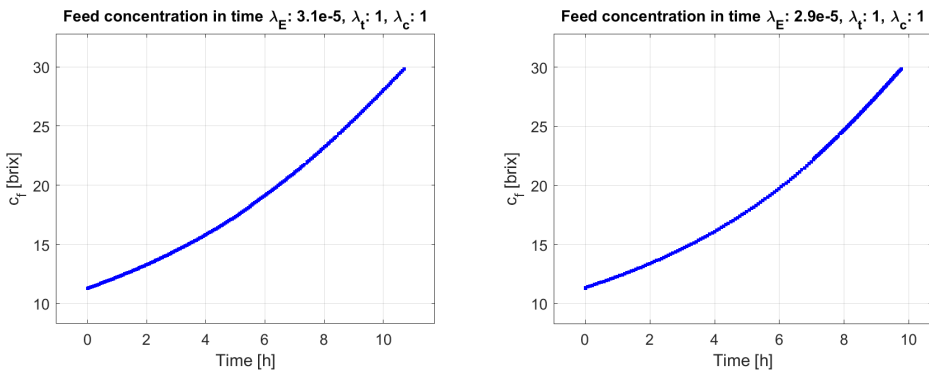


Figure 4.15: Feed concentration: In the first case, it is reached one hour later

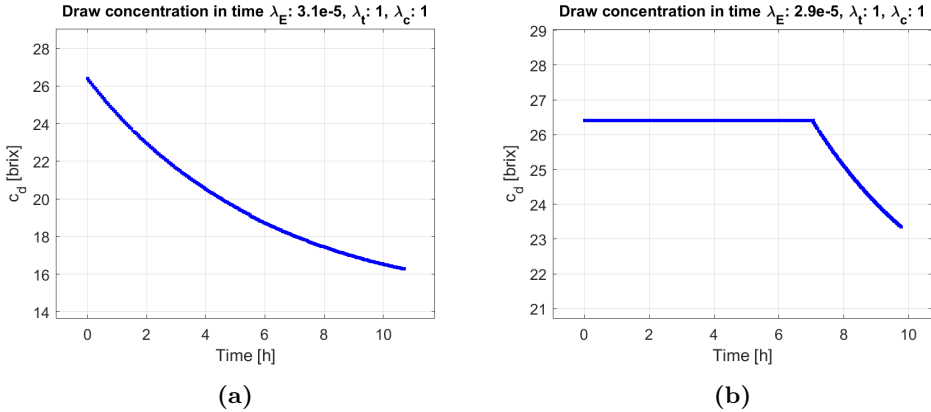


Figure 4.16: Draw tank concentration: Exactly opposite trend as was for draw tank volume (as $c_d \frac{k}{V_d}$).

simulation (Figure (4.16a)).

Now we will compare other features – look at the optimisation problem from a different point of view. To see the influence of given inputs on the output values we will fix λ values and change process features to see the influence of each. This I/O testing will be done firstly in the form of finding the optimal setup for given initial conditions – evaluate it again using time values, total energy consumed and concentration desired 4.5. In the second step we will not search for optimal process setups. We will just simulate the process for given set inputs, one of which is information about when the RO switches on and off. This way we do not simulate optimal solutions, but we can compare the behaviour of the process for different scenarios. This way we can test and observe any setup that we want.

As mentioned above, when testing the setup with changed process variables we can not always easily anticipate how the optimal setup looks like, how it changes when given parameter, initial condition or input is changed. To see how they contribute to results – impact the observed quality parameters, twelve simulations have been conducted. They are shown in 4.5. Parameters and variables impacts of which were tested were: area of FO membrane ($A [m^2]$), area of RO membrane ($B [m^2]$), initial draw solution concentration ($c_{d, \text{init.}} [\text{mass \%}]$), desired concentration of feed to reach ($c_{f, \text{des.}} [\text{Brix}]$) and initial – minimal volume of draw solution ($V_d [L]$). Observed evaluated quality parameters were same as in 4.4.

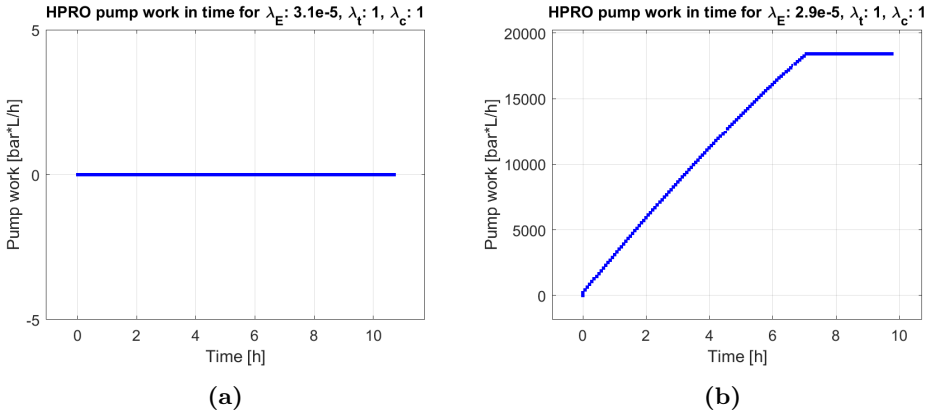


Figure 4.17: Energy in time: Zero for switched of pump, linearly increasing when running.

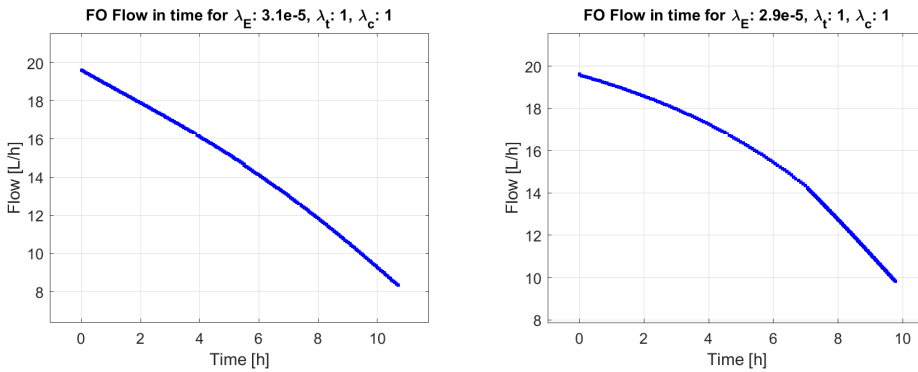


Figure 4.18: Flow through FO membrane: In the second case, it decreases less steeply due to holding c_d at a constant level.

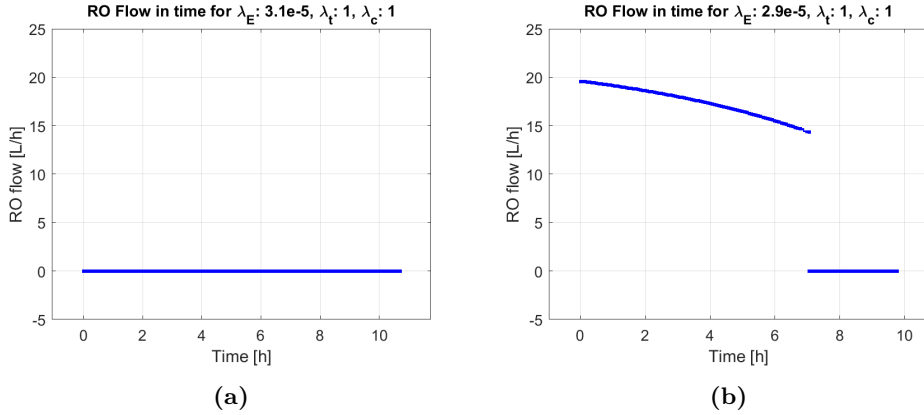


Figure 4.19: RO flow: it decreases moderately with decreasing pressure and constant osmotic pressure.

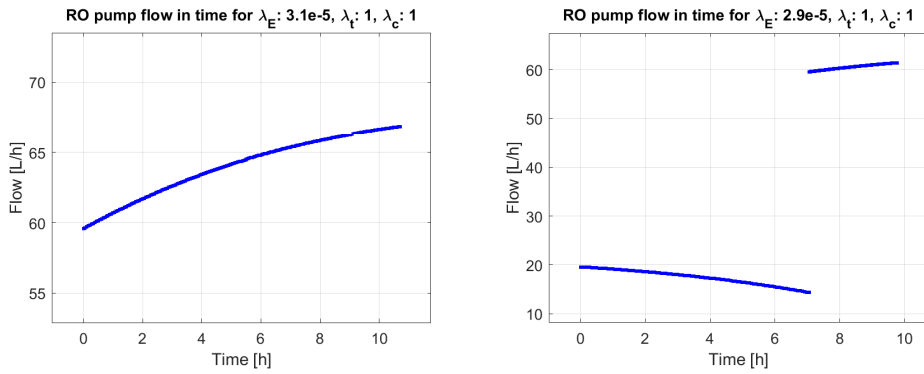


Figure 4.20: Flow to RO pump: To make the process function correctly, the flow to the pump needs to be logically higher than the outflowing extracted water. To minimise energy consumption, the flow is limitedly close to the RO flow (4.19b).

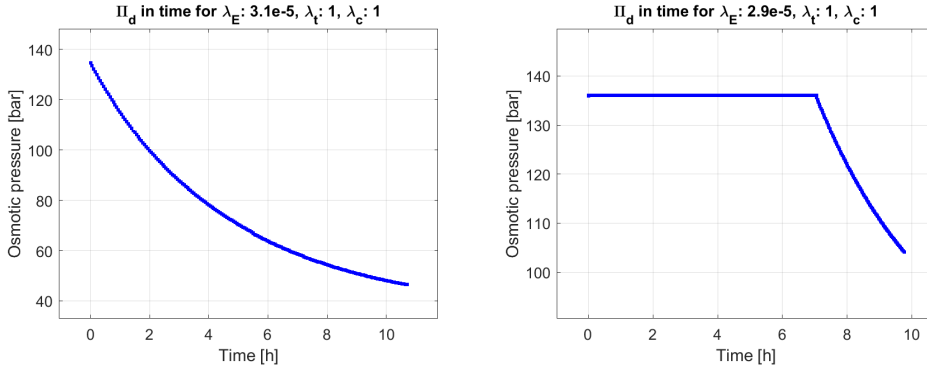


Figure 4.21: Osmotic pressure of draw solution: For the initial concentration of 24 Brix, the corresponding regenerated osmotic pressure is 135 bar. In the first case, with the increasing volume inside the draw tank, it decreases (similarly to feed concentration). In the second scenario, it is held constant while the RO is running. Then, it decreases for the same reason as in the first case.

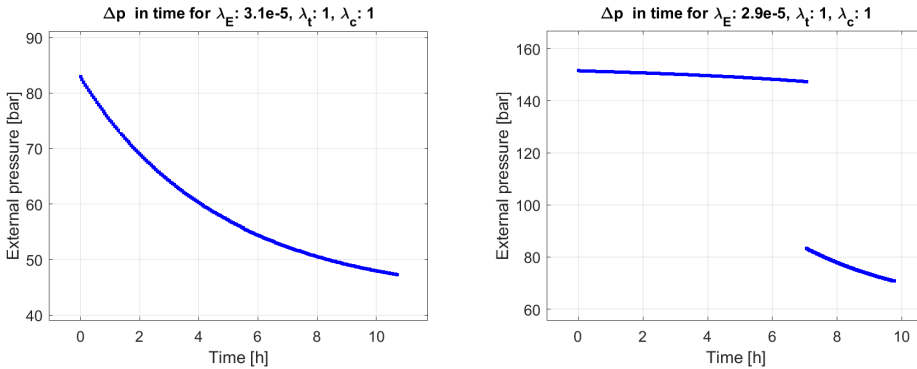


Figure 4.22: External pressure in time: When RO is switched off, it is at zero value, the same as the flow (as no inlet flows to it). When RO is switched on, the RO flux must be positive. For that reason, the pressure is higher than the osmotic pressure of the draw solution. It decreases while the osmotic pressure remains constant, therefore, the RO flow also decreases

When observing the impact of process parameters, it is important to have same λ values in given compared cases. Otherwise would be the results inadequate as different priorities on quality parameters would be applied. First four simulations have been done for $\lambda_E = 1$, $\lambda_t = 2.5 \times 10^4$, $\lambda_c = 1 \times 10^5$, fifth and sixth simulations for $\lambda_E = 1 \times 10^{-3}$, $\lambda_t = 2.5 \times 4$, $\lambda_c = 1 \times 10^7$. Permeability constant R_m remains $0.55 \frac{Lbar}{m^2h}$, initial feed concentration 11.2 Brix and initial feed tank volume 500l as it was in 4.4.

	V_d	A	B	$c_{d, ini.}$	$c_{des.}$	t_1	t_2	t_3	$time$	c_{fin}	E_{sum}
1	250	1	1	15	30	0.2	18.1	4	22	30	9189
2	250	1	1	30	30	1.6	10.4	5.4	17.4	30	30106
3	250	1	1	30	50	3	24.7	0	27.6	49.9	46150
4*	250	1	1	15	50	-	-	-	-	-	-
5**	250	1	1	15	50	0	74	0	74	47.5	267314
6**	250	1	4	15	50	11	60	0	71	7.5	172885
7	250	1	2	15	30	0.6	19.5	1.9	21.4	30	8835
8	250	2	1	15	30	0	9.1	1.95	11	30	9201
9	250	2	4	15	30	0.5	8.8	1.7	11	29.96	8305
10	250	2	6	15	30	0.76	8.6	1.7	11	29.95	8091
11	250	2	30	15	30	2.7	6.7	1.7	11	29.95	5476
12	1000	1	1	15	30	12.6	0	10	22.6	29.9	0

Table 4.5: Table of values of optimised process variables dependent from λ parameters. V_d is in L, membrane areas in m^2 , concentrations in mass%, time in hours, c_{fin} in Brix and E in $[\frac{L}{h}]$. * stands for not conducted simulation, ** represents simulations with different λ parameters (change from (4.4) to (4.4))

First two rows display effect of increased value of $c_{d, ini.}$. Based on theory, the higher is the c_d value, the higher pressure is needed for its regeneration which also represents higher pump work. On the other hand, outcome of higher driving force is higher water separation from feed to draw which results in quicker time of reaching desired concentration. This theoretical hypothesis has shown to be correct based on comparison of second case with the first one. Questionable is whether the difference in less than five hours is worth more than three times higher energy consumption. Again, it depends on our qualitative priorities.

Third and second case represent change in the value of desired concentration. In the third case, $c_{des.}$ was raised to 50 Brix which led to significantly longer time (almost

two times longer) and approximately in 50% higher energy load.

Fourth case shows situation when optimiser brought us information that desired scenario is unfeasible for selected λ values. Based on the parameter change performed (increase of $c_{\text{des.}}$) λ_c needs to be increased to have higher chance of reaching desired concentration level. Simultaneously reducing the weight for energy and time also contributes to achieving this goal. Therefore we have changed it to $\lambda_E = 1 \times -3$, $\lambda_t = 2.5 \times 4$. Thanks to this we have reached desired concentration of 50 Brix. Consequence of this achievement is consumption of almost 70-times more energy than in case 3. To reduce it we might increase λ_E or try changing some of process parameters.

Increase in the size of RO membranes led to a decrease in energy consumption, while the duration and reached concentration remained approximately unchanged in simulations 1 and 7, as well as in simulations 5 and 6. Despite the expected increase in RO flow due to the larger membrane size, it remained constant to maintain the draw regenerated, as observed in figures 4.23a and 4.23b. Similarly, the pump flow also remained constant, as depicted in figures (4.26a) and (4.26b). The primary variable affecting energy consumption was found to be pressure, which decreased from approximately 63 bar to 60 bar, leading to an overall decrease in energy consumption. However, from simulation 1 to 7, the difference was not significant, with only a slight decrease in energy consumption of $354\text{bar} \frac{\text{L}}{\text{h}}$, while from simulation 5 to 6, the energy consumption decreased more significantly, by more than 1.5 times.

In conclusion, the addition of RO membranes allows for the application of lower pressure, to a certain extent depending on other process variables, such as pump flow, FO flow, and RO. It is important to note that reducing pressure is not always feasible due to constraints, as indicated in equation (3.21). The pressure can be lowered only that much to maintain RO flow equal to FO flow. Therefore, the consequent addition of other RO membranes to the already "pressure-minimal" state does not change it anyhow, only increases the material costliness. However, if feasible, the addition of RO membranes can aid in reducing pressure, as shown in the 5th and 6th cases in Table (4.5).

This underscores the importance of our optimisation simulation, as trends do not always manifest consistently due to various influences. Through simulation, we can determine the optimal inputs based on our preferences.

If the goal is to achieve the desired concentration more quickly, increasing the size of the RO membrane may not be as effective, as indicated by the minor change in

time observed in simulations 1 and 7, and in simulations 5 and 6. Instead, adding FO membranes is more impactful.

Doubling the size of the FO membrane results in a corresponding doubling of the FO flux, leading to a halving of the duration for almost the same cost, excluding material needs for the additional membrane. The minor change in energy consumption is due to the process taking half the time for RO operation, with the flow to the RO pump and pressure also increasing. Therefore, while the energy consumption is higher, it is not so significant. Consequently, when aiming to expedite the process while maintaining energy consumption at a similar low level, both FO and RO membranes should be added. This illustrates the aforementioned role of RO membranes in lowering pressure. This is demonstrated in the scenario with 4 RO membranes and 2 FO membranes, in the 9th row of Table (4.5). This simulation, pressure profile of which is illustrated in Fig. (4.25a), was compared to the 8th simulation with 2 FO membranes and only 1 RO in Fig. (4.24c). The pressure is significantly lower, resulting in overall lower energy consumption while preserving the same duration. All of the flows remained at the same level.

To study the effect of RO membrane size, number of units respectively, another simulations have been conducted, from the 10th to the 11th simulation. In these cases, we kept adding RO membranes to the system to confirm our theory that pressure will not decrease as it already reached the limit level in the 9th simulation. We, therefore, anticipated that energy level doesn't change as well, as flows and pressure level do not change. Simulations showed that energy decreased despite preserving RO pump flow and pressure profile at the same pressure level in Fig. (4.25b). The reason why it did so was hidden in the shorter time of the RO pump being switched on. Thanks to the bigger size of RO membrane, it takes shorter time to regenerate it, and therefore it may run lower time to achieve the same result. The energy decrease, however, is not that significant towards the ratio of how much changed the area of RO membrane towards energy difference.

Again, these results are not that straightforward and may be difficult to logically derive. Optimisation reveals them, and that is one of its main incomes.

The last case represented a scenario in which we increased our draw tank volume fourfold. As a result, there was no need to run the RO membrane at all because the dilution rate was very slow due to the significantly increased volume. Consequently, the draw concentration did not decrease rapidly and remained sufficiently high until the desired concentration level was reached.

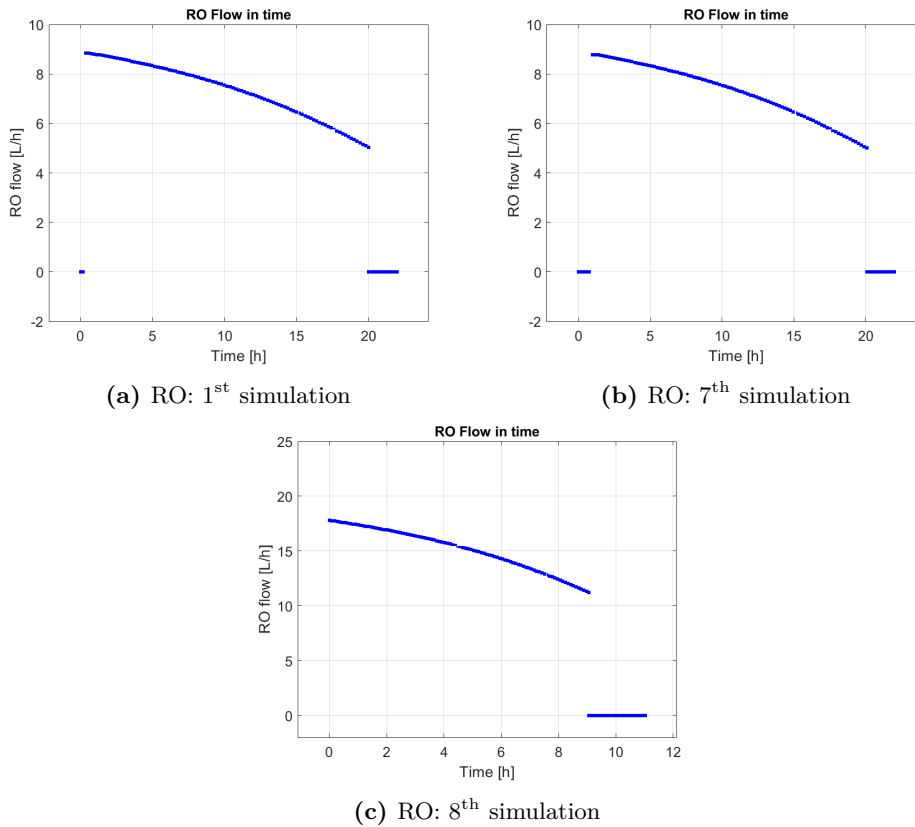


Figure 4.23: RO flow in time: changes with FO flow as a consequence of increase in size of FO membrane.

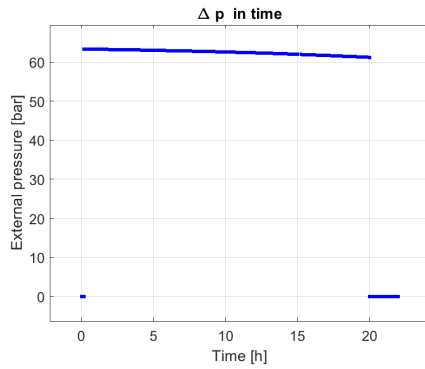
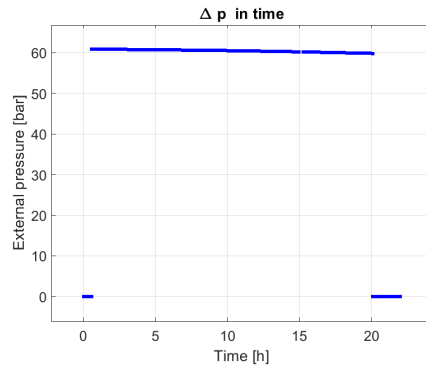
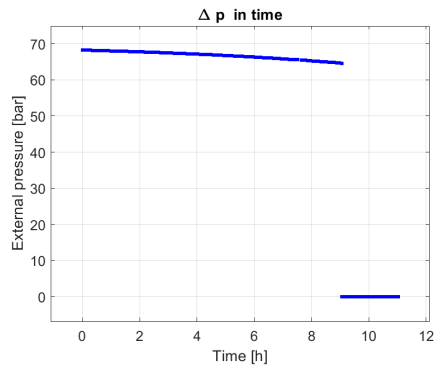
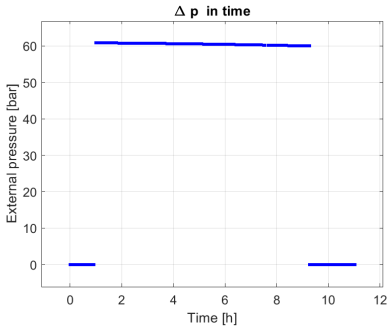
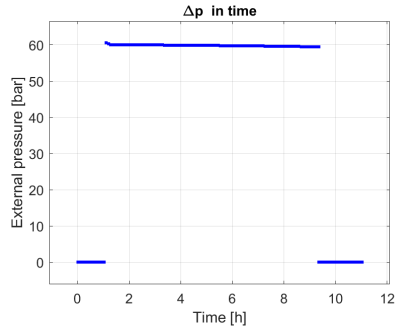
(a) Feed volume in time: 1st simulation(b) Pressure in time: 7th simulation(c) Pressure in time: 8th simulation

Figure 4.24: External pressure is mostly affected by the size of FO membrane and less by the size of RO membrane.

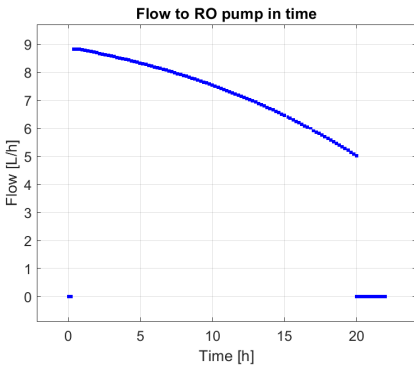


(a) Pressure in time: 9th simulation

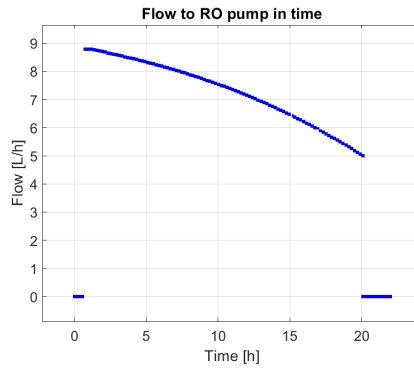


(b) Pressure in time: 10th simulation

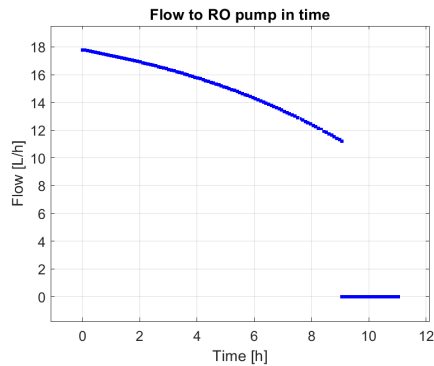
Figure 4.25: External pressure is affected by the size of RO membrane but only to its limit value, which is in this case approximately 60 bar



(a) 1st simulation



(b) Flow: 7th simulation



(c) Flow: 8th simulation

Figure 4.26: Flow proportionally increases with the size of FO membrane.

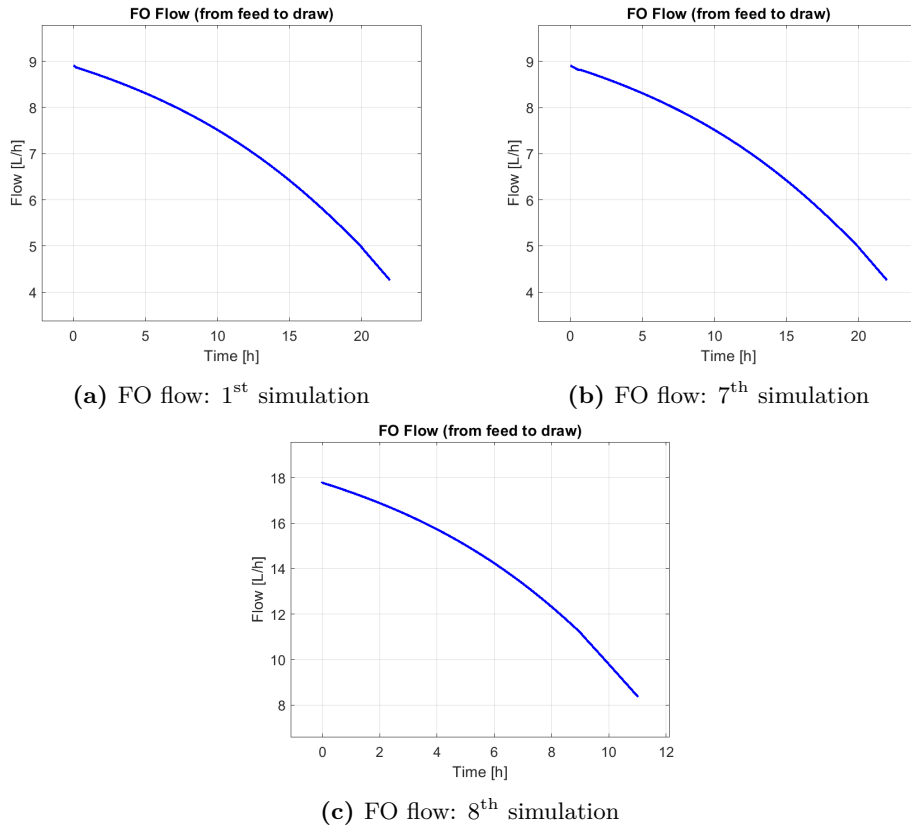


Figure 4.27: FO flow is two-times higher when having two-times bigger FO membrane.

Conclusions and Future Research

Our study focused on optimising the forward osmosis (FO) process, a prerequisite for process optimisation. We derived dynamic equations to describe changes in system states, which are a crucial part of the FO model. Simultaneously, we utilised three optimising approaches to design flux models: white box, grey box, and black box. Our comparison revealed that experimental data are crucial for building trustworthy models. The white box approach serves as a theoretical foundation for estimating non-ideal FO processes, while the grey box method is superior due to its ability to accommodate the non-ideal behaviour of the membrane and uphold mass balances during training, resulting in a more reliable model for state estimation. Conversely, the black box model, by disregarding mass balance theory and solely evaluating model parameters based on flux data, exhibits better anticipation of FO flux. However, for a more realistic representation, we opted for the grey box model for further development.

Within each approach, we explored linear, quadratic, and logarithmic models. While logarithmic models yielded inadequate results in both black and grey box contexts, linear and quadratic models demonstrated similarly accurate performance based on the root mean square error (RMSE) criterion. Given our prioritisation of simpler models over complex ones, we selected the linear model for subsequent analysis.

Having established these flux models, we proceeded to develop a comprehensive model of the entire FO process, including the draw recovery system, and optimised it using the Python environment and CasADi optimiser. By implementing λ values in the loss function, we gained insights into their impact on the process and their manipulation to achieve desired outcomes. We have also explained the way of their initialization aiming to get desired result. Additionally, we explored how changes in process features altered the optimal state, leveraging the optimiser to provide valuable information on handling the RO centrifugal pump, operational pressure, flow rate, running time, and overall process duration. This optimisation process also offered insights into the feasibility of reaching desired outcomes, helping us identify unrealistic scenarios. We

concluded that:

- To get higher final concentration of the feed, more concentrated draw solution should be used. If given desired concentration is reachable using lower concentration of draw solution from the energetic perspective it is not a good solution as it is significantly more energy-consuming. From the temporal point of view it helps to reach the quicker time. But there are more effective time-sparing methods.
- To reduce the energy load, addition of RO membranes, increasing their size respectively, is based on our results, recommended. We found out that by adding them into system we can reduce the pressure value to minimal possible level (which is the one maintaining RO flow equal to FO flow). Addition of RO membranes to the system in which was this lowest pressure state already reached still changes from the energetic point of view despite pressure remains same due to shorter running time of RO pump. The question for our further is whether the energy decrease is worth such increase in material (size, membranes number respectively)
- To reduce the time to reach the desired concentration, addition of FO membranes works best. At the same time it increases energy consumption of RO pump. To keep it on the similar level, addition of RO membranes is recommended.
- Increase of draw solution volume reduces energy consumption as the concentration decreases at a slower rate. That is the reason why RO pump does not need to be switched on that much.
- To get the desired result quickest as possible, RO pump needs to be switched on for the whole time to maintain the draw solution regenerated, thus creating highest FO flow possible.
- To get the lowest final energy value RO pump must be switched off for the whole time. In that case it is zero.

In cases where an optimal state is unnecessary, can be simulation program containing manual entry for input variables such as pressure, flow rate, and RO runtime easily designed out of the optimising program. While these simulations cannot determine optimality, they offer valuable insights into process dynamics and behavior under different conditions, aiding in understanding process trends and identifying incorrect settings.

Moving forward, our focus will extend to the economic aspect of the process, aiming to optimise it from an economic perspective. By considering factors such as energy prices

and material requirements (OPEX, CAPEX), we aim to provide definitive insights into the economically optimal setup.

Bibliography

- [1] Yoram Cohen Aihua Zhu, Panagiotis D. Christofides. Minimization of energy consumption for a two-pass membrane desalination: Effect of energy recovery, membrane rejection and retentate recycling. *Journal of Membrane Science*, 339(14569), 2009.
- [2] Syed Muztuza Ali, Sung-Ju Im, Am Jang, Sherub Phuntsho, and Ho Kyong Shon. Forward osmosis system design and optimization using a commercial cellulose triacetate hollow fibre membrane module for energy efficient desalination. *Desalination*, 510:115075, 2021.
- [3] Joel A E Andersson, Joris Gillis, Greg Horn, James B Rawlings, and Moritz Diehl. CasADi – A software framework for nonlinear optimization and optimal control. *Mathematical Programming Computation*, 11(1):1–36, 2019.
- [4] Alison Cozad, Nikolaos V. Sahinidis, and David C. Miller. A combined first-principles and data-driven approach to model building. *Computers & Chemical Engineering*, 73:116–127, 2015.
- [5] Patel Dhaval et al. Water desalination and wastewater reuse using integrated reverse osmosis and forward osmosis system. *IOP Conference Series: Materials Science and Engineering*, 1146(1), 2021.
- [6] Ravi Jeganes et al. Polymeric membranes for desalination using membrane distillation: A review. *Desalination*, 490(114530), 2020.
- [7] G. Foley. *Membrane Filtration: A Problem Solving Approach with MATLAB*. Cambridge University Press, 2013.
- [8] Mahaveer A. Halakarni, Anita Samage, Ashesh Mahto, Veerababu Polisetti, and S. Nataraj. Forward osmosis process for energy materials recovery from industrial wastewater with simultaneous recovery of reusable water: a sustainable approach. *Materials Today Sustainability*, 2023.

-
- [9] Davide Mattia Kah Peng Lee, Tom C. Arnot. A review of reverse osmosis membrane materials for desalination—development to date and future potential. *Journal of Membrane Science*, 370:1–22, 2011.
- [10] Mohammad Aquib Wakeel Khan, Mohd Muzammil Zubair, Haleema Saleem, Alaa AlHawari, and Syed Javaid Zaidi. Modeling of osmotically-driven membrane processes: An overview. *Desalination*, page 117183, 2023.
- [11] J. Kucera. *Reverse osmosis*. John Wiley & Sons, Ltd, 2015.
- [12] Ibarz A. Ramos M. A. Density of juice and fruit puree as a function of soluble solids content and temperature. *Journal of Food Engineering*, 1998.
- [13] Camilleri-Rumbau M. S., Nguyen X. T., Sanahuja-Embuena V., Frauholz J., Yangali Quintanilla V. A., Tiraferri A., and Helix-Nielsen C. Forward osmosis. *Experimental Methods for Membrane Applications in Desalination and Water Treatment*, 2017.
- [14] Jungwon Choi Sung-Ju Im. New concept of pump-less forward osmosis (fo) and low-pressure membrane (lpm) process. *Scientific Reports* 7, 2017.

Resumé

Naša štúdia je zameraná na modelovanie procesu doprednej osmózy (FO), čo je okrem iného aj kľúčovým prostriedkom pre jeho následnú optimalizáciu. Z materiálových bilancií sme odvodili diferenciálne rovnice popisujúce zmeny stavov systému. Práve na základe nich bol vytvorený základ modelu systému. Pre účely nájdania správneho modelu sme súčasne využili tri vlastne navrhnuté k návrhu modelu intenzity toku cez doprednú membránu: white box, grey box a black box. Porovnaním sme ukázali, že experimentálne údaje sú kľúčové pre vytváranie dôveryhodných modelov. White box slúži ako teoretický základ pre odhad idealizovaného FO procesu, zatiaľ čo grey box metóda vykazuje lepšie predikčné schopnosti reálneho procesu, nakoľko zohľadňuje aj neideálne správanie, počas tréovania zohľadňuje materiálové bilancie, čo vedie k spoľahlivejšiemu modelu odhadu stavov. Naopak, black box prístup tieto hmotnostné bilancie neuvažuje. Parametre modelu toku sú tu určené len na základe nameraných údajov. Ich porovnaním dostávame black box model, dostatočne dobre predikujúci intenzitu toku, no nepresne iné stavy, nakoľko neuvažuje ich dynamické modely. Preto sa za účelom realistickejšej predikcie zvolil model vytvorený grey box metódou.

V rámci každého prístupu sme skúmali použitie lineárneho, kvadratického a logaritmickeho modelu. Zatiaľ čo logaritmicke modely poskytovali neuspokojivé výsledky v prípade black box aj grey box prístupu, lineárne a kvadratické modely preukázali podobnú presnosť predikcie vyhodnotenú metódou najmenších štvorcov (RMSE). Upredenosťením jednoduchšieho modelu pred podobne presným, komplexnejším, sme pre našu ďalšiu prácu vybrali lineárny model určený grey box prístupom.

Po vytvorení modelov toku cez FO membránu a výbere toho najlepšieho sme pokračovali v rozvoji modelu celého FO procesu, už aj vrátane systému na obnovu koncentrácie odťahového roztoku. Proces sme optimalizovali v prostredí Python a jazyka CasADi. Implementáciou váhových parametrov λ do stratovej funkcie sme získali poznatky o ich vplyve na proces a spôsobe ich nastavovania pre dosiahnutie požadovaného optimalizačného cieľa. V druhom kroku sme simulovali, ako zmeny v procesných vlastnostiach ovplyvňujú optimálne nastavenie procesu. Optimalizátor vypočíta optimálne nastavenie vstupov procesu v každom jednom kroku. Výstupom zo simulácie sú okrem optimálnych hodnôt vstupov aj hodnoty optimalizovaných premenných čau, informujúce o tom, kedy je potrebné zapnúť a kedy vypnúť čerpadlo pre zaistenie opti-

málnej prevádzky procesu. Samotná realizovateľnosť procesu pri daných nastavených podmienkach je taktiež užitočnou informáciou, ktorú nám program poskytuje. Detekcia nerealizovateľných nastavení je dôležitou súčasťou z pohľadu praxe. Na základe vykonaných simulácií sme dospeli k viacerým odporozorovaným záverom.

- Pre dosiahnutie vyššej finálnej koncentrácie roztoku je potrebné aplikovať koncentrovanejší odťahový roztok. Ak je požadovaná koncentrácia dosiahnuteľná pomocou nižšej koncentrácie odťahového roztoku, z energetického hľadiska nie je to dobrým riešením používať jeho viac koncentrovanú formu, nakoľko regenerácia koncentrovanejšieho roztoku je energeticky náročnejšia. Z pohľadu dĺžky trvania procesu nám vyššia koncentrácia odťahového roztoku pomáha dosiahnuť kratší čas. Existujú však aj účinnejšie, čas šetriace metódy.
- Na zníženie spotreby energie procesu je vhodné pridať alebo zvýšiť plochu rezverzných membrán. Zistili sme, že ich pridanie do systému spôsobuje zníženie hodnoty externého tlaku čerpadla. Dostatočným zväčšením plochy tejto membrány vieme dosiahnuť jeho minimálnu možnú hodnotu (udržiavajúcej tok cez RO membránu na úrovni toku cez FO). Pridanie RO membrán do systému, v ktorom bol tento limitný tlak už dosiahnutý spôsobilo pokles prevádzkového času čerpadla (nie však času trvania procesu). Otázkou pre naše ďalšie štúdium je, či tento energetický pokles v dôsledku poklesu prevádzkového času stojí za navýšenie materiálnych nákladov procesu.
- Pre účely zníženia prevádzkového času procesu sa najlepšie osvedčilo pridanie, resp. zvýšenie plochy dopredných membrán. To má za následok zvýšenie energetických prevádzkových nákladov čerpadla. V záujme ich udržania na podobnej úrovni je potrebné do procesu pridať RO membrány, resp. zvýšiť ich plochu.
- Zvýšenie objemu odťahového roztoku znižuje energetickú spotrebu procesu, nakoľko sa jeho koncentrácia v dôsledku zvýšeného objemu znižuje pomalšie. To je dôvod, prečo za účelom regenerácie koncentrácie roztoku nie je potrebné mať čerpadlo zapnuté po rovnako dlhý čas.
- Na čo najrýchlejšie dosiahnutie požadovaného výsledku je potrebné mať koncentráciu odťahového roztoku po celý čas maximálnu a teda čerpadlo musí byť zapnuté nepretržite od začiatku až po dosiahnutie výslednej koncentrácie. Pretože tým sa vytvára najvyšší možný tok cez FO membránu.
- Na dosiahnutie najnižšej konečnej energetickej hodnoty musí byť čerpadlo RO vypnuté po celý čas. Vtedy je energetická spotreba nulová. Čas trvania takéhoto procesu je výrazne dlhší.

V prípadoch, kedy nie je potrebné hľadať optimálny stav, môže byť FO proces simulovaný bez súčasného hľadania optimálneho nastavenia. Zadaním konkrétnych hodnôt vstupov, ktorými sú tlak, prietok a čas prevádzky, ľahko navrhnutý pomocou jednoduchých zmien v optimalizačnom programe. Hoci tieto simulácie neurčujú optimálne nastavenie, poskytujú cenné informácie o dynamike procesu, jeho správaní sa pri rôznych podmienkach, a to pomáha pochopiť trendy, prípadne identifikovať nesprávne nastavenia.

V ďalšom kroku bude naša pozornosť upriamená na štúdium ekonomického aspektu procesu, s cieľom optimalizovať ho práve z tejto ekonomickej perspektívy. Zohľadnením faktorov akými sú napríklad cena energie, požiadavky na materiál (OPEX, CAPEX) sa snažíme poskytnúť finálne poznatky o optimalizácii procesu doprednej osmózy.